Thesis for The Degree of Doctor of Philosophy

Mercury Decontamination of Aqueous Solutions via Electrochemical Alloy Formation

Vera Roth

Department of Physics
Chalmers University of Technology
Gothenburg, Sweden, 2025

Mercury Decontamination of Aqueous Solutions via Electrochemical Alloy Formation

Vera Roth

ISBN 978-91-8103-179-9
Doktorsavhandlingar vid Chalmers tekniska högskola, Ny serie nr 5637.
ISSN 0346-718X

Division of Chemical Physics
Department of Physics
Chalmers University of Technology
SE-412 96 Gothenburg,
Sweden

Cover: Electrochemical alloy formation between Hg (blue) and Pt (gray).

Printed by Chalmers Digitaltryck,
Gothenburg, Sweden 2025.

Mercury Decontamination of Aqueous Solutions via Electrochemical Alloy Formation

Vera Roth
Department of Physics
Chalmers University of Technology

Abstract

Mercury is a global pollutant that poses severe risks to human health and ecosystems. It is a naturally occurring element released into the environment through natural processes, however, human activities have drastically increased its emissions, with water serving as a key medium for its mobility and dispersal. Effectively addressing mercury contamination in water is crucial for mitigating its widespread impact and safeguarding all living beings from its toxic effects. Current technologies for mercury removal from aqueous solutions are far from optimal, calling for the development of more effective removal methods. This thesis investigates a novel removal method based on electrochemical alloy formation between mercury ions in solution and a metal, such as platinum. Key aspects are examined, such as the reaction mechanisms, energetics, and the regeneration process of platinum electrodes. In addition, the method's potential for practical applications is evaluated by demonstrating efficient mercury removal from dental clinic wastewater and industrial sulfuric acid derived from smelting. This research addresses the limitations of current techniques and establishes a strong foundation for further investigation and optimization of electrochemical alloy formation as a method for mercury removal. With continued development, this method holds significant potential for reducing global mercury pollution and protecting human health and ecosystems.

Keywords

Mercury Removal; Electrochemistry; Platinum; Mercury; Alloy Formation

List of Publications

This thesis is based on the following publications:

Paper I

Feldt, E., Järlebark, J., **Roth, V.**, Svensson, R., Gustafsson, P. K., Molander, N., Tunsu, C., and Wickman, B.
"Temperature and Concentration Dependence of the Electrochemical $PtHg_4$ Alloy Formation for Mercury Decontamination"
Separation and Purification Technology **319**, 124033 (2023).

Paper II

Roth, V., Valter-Lithander, M., Strandberg, L., Bilesan M. R., Järlebark, J., Jamroz, J., and Wickman, B.
"On the Mechanism and Energetics of Electrochemical Alloy Formation between Mercury and Platinum for Mercury Removal from Aqueous Solutions"
Electrochimica Acta **507**, 145137 (2024).

Paper III

Roth, V., Järlebark, J., Ahrnens, A., Nyberg, J., Salminen, J., Vollmer, T. R., and Wickman, B.
"Mercury Removal from Concentrated Sulfuric Acid by Electrochemical Alloy Formation on Platinum"
ACS ES&T Engineering **3**, 823 (2023).

Paper IV

Roth, V., Ernbring, H., and Wickman, B.
"Mercury Decontamination of Dental Clinic Wastewater using Electrochemical Alloy Formation"
ACS ES&T Water. In revision (2025).

Author Contributions

Paper I

Responsible for the finalization of the manuscript, which included writing parts of the text, refining figures, and collaborating with co-authors on the final version.

Paper II

Contributed to the design of the experimental setup and protocol and was responsible for preparing the working electrodes. Conducted EQCM-D measurements and ICP-MS analyses, wrote and prepared the first draft of the manuscript, which was finalized together with the co-authors.

Paper III

Contributed to the design of the experimental setup and protocol and was responsible for preparing the working electrodes. Conducted EQCM-D measurements and ICP-MS analyses, wrote and prepared the first draft of the manuscript, which was finalized together with the co-authors.

Paper IV

Contributed to the design of the experimental setup and protocol. Co-wrote and prepared the first draft of the manuscript, which was finalized together with the co-authors.

List of Acronyms

AAS	–	Atomic Absorption Spectroscopy
ASGM	–	Artisanal and Small-Scale Gold Mining
CE	–	Counter Electrode
CV	–	Cyclic Voltammetry
DALYs	–	Disability Adjusted Life Years
DFT	–	Density Functional Theory
DMA	–	Direct Mercury Analyzer
DMeHg	–	Dimethylmercury
ECSA	–	Electrochemical Surface Area
EQCM	–	Electrochemical Quartz Crystal Microbalance
EQCM-D	–	- with Dissipation Monitoring
HER	–	Hydrogen Evolution Reaction
ICP-MS	–	Inductively Coupled Plasma Mass Spectrometry
MeHg	–	Methylmercury
ORR	–	Oxygen Reduction Reaction
RE	–	Reference Electrode
RHE	–	Reversible Hydrogen Electrode
SEM	–	Scanning Electron Microscopy
SHE	–	Standard Hydrogen Electrode
WE	–	Working Electrode
XRD	–	X-ray Diffraction

Contents

Chapter 1

Introduction

Environmental pollution is one of the most pressing and rapidly growing challenges facing the modern world. Across the globe, toxic chemicals are continuously released into the environment, causing detrimental impacts on soil, air, and, perhaps most critically, water. Water is essential to all forms of life, and the consequences of its pollution are both far-reaching and devastating. Contaminated water affects entire ecosystems, and in many cases becomes a vector of disease and death [1–3].

Mercury (Hg) is a highly toxic heavy metal and is recognized as one of the most severe environmental threats globally, affecting tens of millions of people. It is estimated that Hg is surpassed only by lead and radionuclides in terms of the number of people impacted, the severity of exposure, and the geographical extent of its contamination [4]. Recognizing the gravity of the issue, *the World Health Organization* (WHO) has classified Hg as one of the top ten chemicals of major public health concern [5]. Furthermore, the *Minamata Convention on Mercury*, a landmark global environmental treaty, has been established to combat Hg pollution through coordinated international efforts, aiming to mitigate the devastating and far-reaching effects of Hg on both the environment and human health [6].

Hg occurs naturally in the environment and is released into the atmosphere through natural processes such as rock weathering and geothermal activity [7]. However, estimates suggest that Hg emissions from anthropogenic sources exceed natural emissions by more than one order of magnitude, with over 2000 tonnes emitted annually [8, 9]. Human activities that contribute to the Hg emissions, include mining, fertilizer production, waste incineration, and disposal. From human activities alone, an estimated total of 1,540,000 tonnes of Hg was released between the years 1850 – 2010, with 470,000 tonnes directly emitted into the atmosphere and 1,070,000 tonnes discharged into land and water [9]. These estimates are likely significantly underestimated, as a substantial portion of Hg emissions remains unaccounted for, in particular from unregulated and illegal mining operations [10, 11].

Once Hg is emitted into the environment, it can travel vast distances, extending its impact far beyond the original emissions source. After entering the atmosphere, Hg can be deposited onto surfaces such as land and water, where it can subsequently be re-emitted back into the atmosphere. This ability to cycle continuously between atmosphere, land, and water allows Hg to remain active in the environment, where it can persist for millennia, remaining mobile and toxic until its ultimately bound in deep ocean sediments or subsurface soils [12, 13]. Water is a major contributor to the re-emission of Hg, playing a key role in its mobility and distribution in the environment [14]. Furthermore, once Hg enters aquatic ecosystems, it bioaccumulates in organisms and subsequently biomagnifies up the food chain, posing significant risks to all forms of life [15]. Addressing Hg pollution in water is, therefore, of high importance.

There is an urgent need to develop new effective strategies to manage and mitigate the impacts of Hg pollution [16]. Current established methods for Hg removal from aqueous solutions, although functional, are far from optimal. The most commonly used methods include techniques such as adsorption, filtration, ion exchange, and precipitation. Each of these methods, depending on the specific context and application, has its own advantages and disadvantages [16, 17]. Common limitations can include low selectivity for Hg, high capital cost and energy consumption, technical complexity and the generation of secondary waste. In addition, the effectiveness of these methods can often be highly sensitive to the pH of the solution, and notably, no existing method has been proven effective for Hg removal from concentrated acids [16, 18].

A novel method for Hg removal from aqueous solutions was recently introduced, which involves electrochemical alloy formation between Hg ions in solution and a metal surface, such as platinum (Pt) [19]. This technique has the potential to address the limitations of existing Hg removal methods, offering a more effective and efficient method for various applications, including the treatment of natural water, wastewater, and concentrated acid [19–22]. With further research and optimization, this electrochemical method could be developed into a scalable and practical solution, helping to mitigate the impact of this toxic heavy metal on our planet.

1.1 Scope of the Thesis

This thesis presents research and findings aimed at advancing the understanding of electrochemical alloy formation as a method for Hg removal from aqueous solutions. Through electrochemical experiments and detailed analysis, the reaction mechanisms and energetics of the processes involved in alloy formation for Hg removal and alloy dissolution for electrode regeneration are thoroughly investigated. In addition, the potential of this method for practical applications is explored by demonstrating its effectiveness in removing Hg from two challenging matrices: dental clinic wastewater and concentrated sulfuric acid derived from smelting.

Chapter 2 provides a background on Hg pollution, detailing its sources, pathways, impacts on human health and ecosystems. In addition, current removal methods from aqueous solutions are reviewed and summarized. Chapter 3 introduces the fundamentals of electrochemistry, focusing on the structure and workings of a basic electrochemical cell. In addition, this chapter explains the underlying thermodynamics and kinetics of the electrochemical processes relevant to this research. Chapter 4 outlines the principles and mechanics of the electrochemical alloy removal method for Hg removal, as well as describing the experimental setups and analytical techniques used. Chapter 5 discusses and elaborates on results presented in **Paper I** through **IV**. The discussion focuses on key findings, their implications, and the potential of the electrochemical removal method for practical applications. Finally, Chapter 6 concludes the thesis, summarizing the main outcomes and providing suggestions for future research directions.

Chapter 2

Mercury

2.1 Sources and Pathways of Pollution

Hg is a naturally occurring element widely distributed in the earth's crust, oceans and atmosphere [23]. Despite its natural occurrence, human activities have significantly elevated levels of Hg pollution in the environment. In recent decades, efforts have been made to reduce Hg emissions. However, the persistence of Hg in the environment still remains a significant concern [8].

Sources of Hg pollution can be broadly classified into two main categories [14]: natural and anthropogenic, which can be further subdivided into primary and secondary sources. Primary natural sources, such as volcanoes, rock weathering, and geothermal activities, are estimated to release approximately 80 – 600 tonnes of Hg annually. In stark contrast, primary anthropogenic sources, originating from human activities, emit around 1900 – 2900 tonnes of Hg into the environment annually [14]. It is further estimated that a total of 1,540,000 tonnes of Hg had been released by human activities by 2010, with 70% of these emissions occurring after 1850 [9]. This notable increase in Hg emissions can be linked to the industrial revolution and the rapid expansion of industrial processes such as mining, fossil fuel combustion, and waste incineration [24]. Today, primary human activities increasing the total pool of Hg in the environment are processes such as burning of fossil fuels, artisanal and small-scale gold mining (ASGM), mining of non-ferrous metals, cement production, and waste disposal [7, 25]. However, it has been reported that estimates of Hg emission are likely conservative, as a significant proportion of emissions remains largely unaccounted for, in particular from unregulated and illegal mining operations, such as ASGM [11]. ASGM is believed to contribute significantly more to global Hg emissions than previously estimated. Recent studies indicate that its actual contribution exceeds one-third of all anthropogenic Hg emissions to the atmosphere, with estimates reaching around 1000 tonnes annually [10].

Once Hg is released into the environment, it can travel vast distances via air and water [15]. Hg emitted in one part of the world can be transported across continents and reach remote areas, such as the Arctic [26, 27]. After being released into atmosphere, Hg can be deposited onto various environmental surfaces, such as soil, vegetation, and water. Within these environments, Hg undergoes continuous cycling, as these surfaces can repeatedly re-emit Hg back into the atmosphere. Hg can persist in the environment for thousands of years, remaining mobile as it cycles repeatedly between re-emission and deposition until it is eventually bound in its final forms, such as in deep ocean sediments or subsurface soils [14, 28]. This re-emission of Hg can originate from both primary anthropogenic and natural sources, and is often categorized as a secondary emission source. In short, primary emissions increase the overall Hg pool in the environment, while secondary emissions redistribute it within ecosystems, resulting in widespread pollution of both terrestrial and aquatic environments [8, 14]. Overall, it is estimated that around 8000 tonnes of Hg are released annually into the atmosphere from all sources, with around 7000 tonnes deposited onto land and water. As a result, an estimated 950,000 tonnes of Hg have accumulated in soils and 310,000 tonnes in oceans [8]. A more detailed breakdown of different Hg sources, as well as estimated emissions, is depicted in Fig. 2.1.

In the environment, Hg can exist in various forms, with each playing a distinct role in Hg's environmental cycling and exhibiting complex behaviors that are not yet fully understood [15, 29]. To simplify this highly intricate system, the predominant form of Hg found in the atmosphere is elemental Hg (Hg^0). In the atmosphere, Hg^0 can be oxidized to ionic Hg, primarily in its divalent form (Hg^{2+}), or attach to other particles to form particulate-bound Hg (Hg(p)). In addition, Hg^{2+} can form a metal-metal bond, generating $Hg_2{}^{2+}$, however, this species is highly unstable and rapidly dissociates into Hg^{2+} and Hg^0. While Hg^{2+} can also be reduced back to Hg^0, this process has been shown to play less significant role in atmospheric Hg cycling compared to the oxidation of Hg^0. From the atmosphere, Hg^0 can be deposited onto land or water through dry deposition, which primary involves direct settling of Hg^0 or Hg(p), and wet deposition, where Hg^{2+} is predominantly deposited through precipitations such as rain, snow, or fog. Once deposited, Hg^0 can undergo further transformation, converting into other forms of Hg species, such as Hg^{2+} and Hg(p), or simultaneously be re-emitted back into the atmosphere. In addition to these processes, Hg can undergo methylation, converting Hg^0 or Hg^{2+} into organic Hg compounds, such as methyl Hg (CH_3Hg^+, MeHg) and dimethyl Hg ($(CH_3)_2Hg$, DMHg). The amount and ratio of different Hg species, as well as how readily they oxidize or reduce, can depend on various environmental factors, such as temperature, moisture, pH values, redox states, and the presence of other chemical species that can interact with Hg. These factors can vary significantly between atmospheric, terrestrial, and aquatic systems, leading to very distinct behaviors and transformation pathways for Hg in each environment [13, 29].

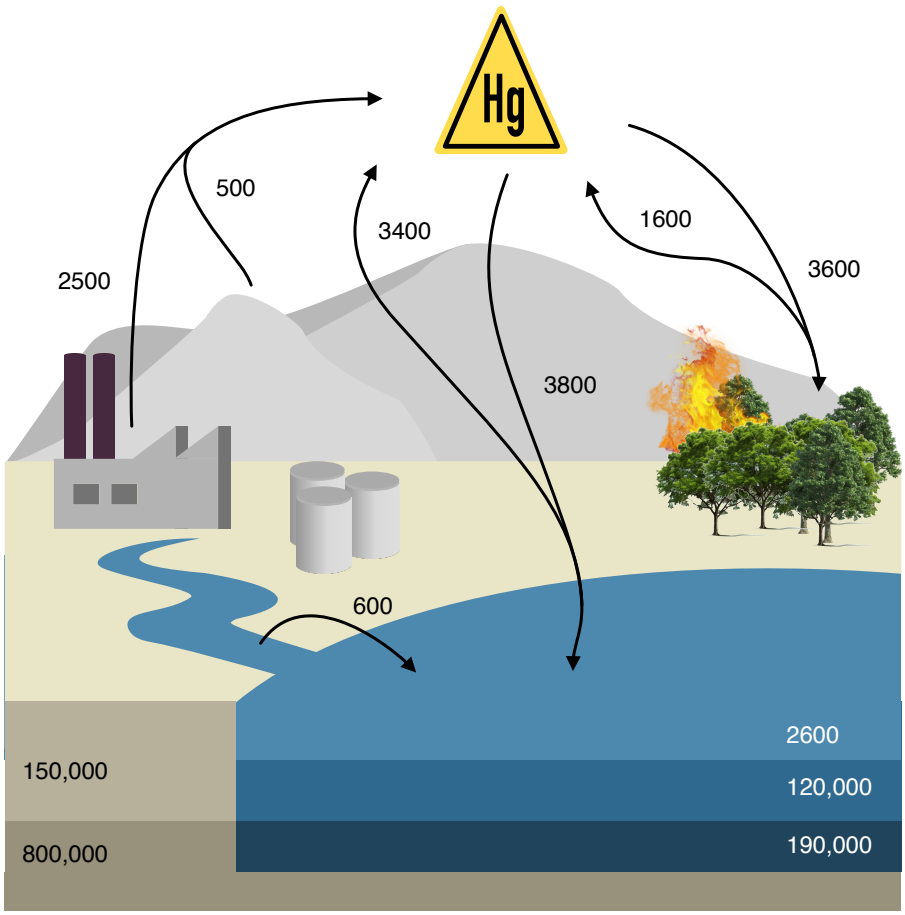

Figure 2.1: An annual cycle of estimated Hg emissions (in tonnes), deposition, and re-emission in the environment. In addition, the total Hg estimated to be accumulated in various reservoirs is shown, including organic and mineral soil, as well as surface ocean, intermediate water, and deep water.

2.2 Environmental Risks and Toxicity

Hg is an element with unique physical and chemical properties that contribute to its complex and extensive effects on ecosystems and all forms of life. Its high toxicity, mobility, and ability to bioaccumulate and biomagnify through the food chain make it one of the most concerning environmental pollutants [30]. Aquatic ecosystems are particularly vulnerable to the impacts of Hg pollution. Once Hg enters bodies of water, it can travel up the food chain, becoming progressively more concentrated in fish, birds, and mammals. Even relatively low concentration of Hg in water can evolve into a more menacing threat, e.g., the concentration of Hg in tissues of top predators, such as whales and seals, can exceed million times the levels in their surrounding waters [8, 13]. The effects on these species can be severe, leading to behavioral changes, reproductive issues, and in extreme cases, population decline and extinction. The toxic effects of Hg are not only limited to the top of the food chain. Hg is toxic to all forms of life, disrupting ecosystems at every level, from microorganisms to apex predators [31–33].

The adverse effects of Hg pollution extend beyond wildlife to human populations [34]. Humans are primarily exposed to Hg through the consumption of contaminated food and water, as well as occupational exposure to Hg vapor in certain industries such as mining, manufacturing of Hg-containing products, dental amalgam restorations, and waste incineration. In addition, humans can be exposed, though to a lesser extent, to Hg salts found in cultural medicinal practices, cosmetics, and house paints [35–38]. The impacts of Hg exposure in the general population can be broadly categorized into short-term and long-term effects, depending on the duration and intensity level of exposure, as illustrated in Fig. 2.2. Short term exposure to high levels of Hg^0 vapor can have immediate and severe health consequences. Initial symptoms are often flu-like and can include soar throat, coughing, chest pain, nausea, headaches, and vision problems. In severe cases, the Hg poisoning can lead to respiratory and kidney failures, which may even prove fatal [35]. To a lesser extent, exposure to Hg^0 can occur through inhalation of Hg vapor released from dental amalgams, where Hg^0 is absorbed through the respiratory system. Ingesting Hg^0 is generally not considered a high risk to healthy individuals, as it is poorly absorbed in the gastrointestinal tract. Similarly, Hg salts, are typically non-volatile solids and rarely cause poisoning by inhalation. Long-term effects of Hg exposure primarily stem from chronic exposure to lower levels of MeHg mainly through consumption of contaminated seafood [35]. Seafood contains significantly higher levels of MeHg compared to other food such as, grain, vegetables, dairy products, and poultry, although trace amounts of MeHg can still be present. MeHg is a strong neurotoxin that can cause lasting neurological and cardiovascular damage, potentially leading to life-threatening conditions [39, 40]. One of the most alarming aspects of long-term Hg exposure is its impact on developing fetuses and children. The nervous system of a developing child is particularly vulnerable to Hg, which can result in cognitive impairments and learning disabilities [39, 41, 42].

In response to the devastating effects of Hg, various global policies and initiatives have been set to raise public awareness and mitigate Hg pollution on a global scale. The environmental organization *Pure Earth* together with *Green Cross* have defined Hg as one of the world's most toxic threats, alongside lead, radionuclides, chromium, pesticides and cadmium [4]. It is reported that approximately 20 million people worldwide are at risk from Hg exposure, with an estimated 1.5 million years of healthy life (Disability Adjusted Life Years, DALYs) lost due to its effects. Furthermore, WHO has recognized Hg as one of the top ten chemicals of public health concern, listed alongside chemicals such as arsenic, lead, asbestos, and hazardous pesticides [5]. As a result, both WHO and the *European Union* (EU) have implemented strict regulations for Hg concentration in drinking water, where only water with Hg concentration below 6 µg/L and 1 µg/L, respectively, is considered safe for human consumption [43, 44]. In 2017, the *Minatamata Convention on Mercury* came into force, addressing the widespread Hg pollution by human activities through coordinated global efforts. The convention aims to reduce Hg emissions, limit its supply and trade, and mitigate its harmful effects on human health and the environment [6]. It is named after the devastating Hg poisoning incident in Minamata Bay, Japan, which also originated the terms *Minamata disease* and *Dancing cat disease* [45]. First identified in 1956 and traced back to industrial wastewater contaminated with MeHg, which was discharged into the bay [42]. Within the bay, MeHg bioaccumulated and biomagnified in aquatic organisms and fish, which were then consumed by the local population. This resulted in severe Hg poisoning, causing neurological disorders, disabilities, and fatalities [46]. Even today, many individuals continue to suffer from the long-term consequences [47].

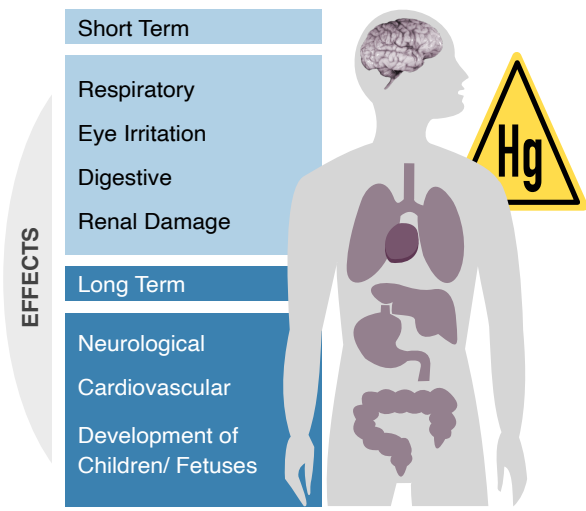

Figure 2.2: Main short term and long term health effects of human exposure to Hg.

2.3 Removal Methods

Various strategies have been employed to mitigate Hg pollution, such as Hg capture technologies, phasing out of unnecessary Hg-containing products and establishing robust waste management systems. Despite these efforts, Hg continues to be pervasive in the environment [4, 6, 48]. Existing methods for Hg decontamination of aqueous solutions, such as natural water, wastewater, and industrial effluent, are far from ideal and are often proven ineffective under certain conditions, particularly in highly acidic and corrosive conditions [16, 49]. Current removal methods include adsorption, coagulation and flocculation, flotation, ion exchange resins, membrane filtration and chemical precipitation. Each of these techniques has its own set of advantages and limitations, as detailed in Table 2.1. Notably, the main limitations can include high energy demands and operational costs, low selectivity, and a strong dependency on pH levels [16]. Currently, no commercial method has the ability to operate in concentrated acid, e.g., effective sulfide precipitation can require a pH range of 7 – 9, and the optimum pH for adsorption methods is typically between 4 – 5 [50, 51]. Furthermore, most materials used for ion-exchange, membrane separation, and adsorption methods, degrade when exposed to concentrated acids [16]. The development and implementation of new and improved methods for Hg removal from various aqueous solutions is therefore urgently needed. Electrochemical alloy formation, although still in its early stages of development, presents a promising alternative to current established methods [19]. A comparison of the primary advantages and drawbacks of the electrochemical method relative to the other methods, is also presented in Table 2.1. The method's fundamental principles, as well as its advantages and limitations, are explored in greater detail in the following chapters.

Adsorption is a widely used technique for Hg capture and has shown to be particularly effective in treating flue gas and wastewater. However, the Hg removal capacity can vary significantly depending on the type of adsorbent used. Activated carbon is one of the most commonly used adsorbents due to its high efficiency and availability. However, more cost-effective alternatives, such as agricultural waste-based adsorbents and biosorbents, including microbes, algae, and non-living biomass, have been proposed. The efficiency of adsorption can be influenced by factors such as pH, temperature, and the saturation level of the adsorbent. The method demonstrates limited selectivity for Hg, as other ions and pollutants can also be adsorbed. In addition, the regeneration of the adsorbent material, while not always possible, can be expensive and can result in material degradation [16, 18, 51].

Coagulation and flocculation is an alternative method commonly employed for the treatment of wastewater, primarily targeting Hg ions. These processes involve the addition of a coagulant, which reacts with Hg ions to form larger, insoluble particles, known as flocs. The method is simple in its operation and cost effective, making it particularly appealing for large-scale applications. However the resulting particles, flocs, must be removed through additional complementary methods, such as precipitation or filtration. This additional step

increases the complexity of the treatment process, requiring additional chemicals and exhibiting low selectivity, as other ions may also become incorporated into the flocs, reducing the overall efficiency of Hg removal [18, 52].

Flotation is another method used to extract pollutants from water, with ion flotation being particularly effective for the removal of heavy metal ions, such as Hg. This process involves the addition of an amphiphilic surfactant to the water, which interacts with Hg ions and attaches them to air bubbles. These air bubbles rise to the surface, thus allowing Hg to be separated from the water. The method has demonstrated high selectivity and efficiency, however these factors can be strongly dependent on pH. In addition, the costs of installation and maintenance can be high, limiting the application of this method in some settings [18, 52, 53].

Ion exchange treatment, a process in which Hg ions are swapped with other non-toxic cations within an ion exchange resin, can offer a fast and efficient approach to Hg removal. This method is particularly valuable for treating larger volumes of solutions containing low concentrations of Hg ions. However, the efficiency of this process is heavily influenced by factors such as pH, temperature, and contact time. In addition, due to rapid resin saturation, this method is less suitable for higher concentrations of Hg and tends to generate large amounts of secondary waste [18, 54].

Membrane filtration includes a variety of technologies that utilize different types of membranes, in particular for wastewater treatment for ionic Hg or Hg(p). Ultrafiltration is one such technology, where low pressure is applied to force water through a membrane, separating molecules and colloidal particles larger than the membrane's pore size. In this process, ligands are often introduced to the water to form larger chelates with Hg, which can then be filtrated out. However, due to the substantial cost associated with these ligands, their recovery and reuse are crucial to make this process economically feasible. In addition, other membrane filtration techniques have been reported to experience rapid clogging of the membranes and removal efficiencies affected by pH [16, 18, 52].

Precipitation is one of the most commonly used methods for industrial wastewater treatment. This process involves the addition of a chemical, typically a sulfide salt, to the water, which leads to the formation of insoluble precipitates such as Hg sulfide (HgS). The effectiveness of this technique is highly dependent on pH and can lack selectivity for Hg, as other metals can also precipitate alongside Hg, complicating the Hg removal process [16, 52].

Table 2.1: Methods for removing Hg from aqueous solutions, along with their main advantages and limitations [16, 18], as well as potential advantages of electrochemical alloy formation [19–22, 55].

Method	**Advantages**	**Limitations**
Adsorption	Simple operation High removal rate	High capital cost Low selectivity Secondary waste pH dependent
Coagulation/ Flocculation	Simple process Low capital cost High removal efficiency	Chemical consumption Secondary waste Ineffective at low/high conc. Low selectivity pH dependent
Flotation	High selectivity High removal efficiency	High capital cost High energy consumption pH dependent
Ion exchange	Simple operation Time efficient High removal efficiency	High capital cost Low selectivity pH dependent
Membrane filtration	Simple process Time efficient Effective at low conc.	High operation cost High energy consumption pH dependent Membrane clogging
Precipitation	Simple operation Cost efficient High removal rate	Low selectivity Ineffective at low conc. Secondary waste pH dependent
Electrochemical alloy formation	Simple operation High removal efficiency High selectivity Effective at low/high conc. pH independent Low energy consumption	Early development stages

Chapter 3

Electrochemistry

3.1 The Electrochemical Cell

Electrochemistry is a field of science that spans a vast range of phenomena and extends beyond the traditional boundaries of physics and chemistry. It explores the relationship between electricity and chemical reactions and has proven instrumental in many technological advancements, with applications ranging from battery technology and fuel cells to electroplating and corrosion processes [56]. Moreover, electrochemistry offers new possibilities for environmental remediation, particularly in the removal of hazardous substances, such as toxic heavy metals [19].

At the core of electrochemistry are oxidation-reduction (redox) reactions, where electrons are transferred from one chemical species, the reducing agent, to another, the oxidizing agent. These reactions can be either spontaneous, generating electrical energy as in galvanic cells, or non-spontaneous, as in electrolytic cells, where electrical energy is used to drive a desired chemical reaction. A simple electrochemical cell consists of two electrodes, the anode, and the cathode, connected by an internal ionic pathway provided by an electrolyte, and an external electric connection to an electric load/generator. Each electrode serves as the location for one of two half-reactions that occur at the interface between the electrode and the electrolyte. Electrons flow from the anode, where oxidation occurs, to the cathode, where reduction takes place. The electrolyte enables the flow of ions needed to balance the charge and requires high ionic conductivity to minimize solution resistance and prevent resistive heating. Electrolytes can be in solid or liquid form, with aqueous electrolytes being the most commonly used and extensively studied. Together with the choice of electrode materials, the composition of the electrolyte plays a crucial role in efficiency and specificity of the electrochemical process [56].

The cathode or the anode can be referred to as either the working electrode (WE) or the counter electrode (CE), depending on the study and cell setup. The WE is where the half-reaction of interest occurs, while the CE facilitates charge balance and completes the electrical circuit. When a potential is

applied between the WE and CE, the resulting current response is measured. Alternatively, when a current is applied, the resulting potential response is recorded. Since the current flows through the counter electrode (CE), its potential can shift, making it difficult to accurately determine the absolute potential of the working electrode (WE). To address this, a third electrode, known as the reference electrode (RE), is introduced. The potential of the WE is then measured relative to the RE. Since no significant current passes through the RE, the current is measured exclusively between the WE and CE. These two setups, two-electrode and three-electrode configurations, are shown in Fig. 3.1 [56].

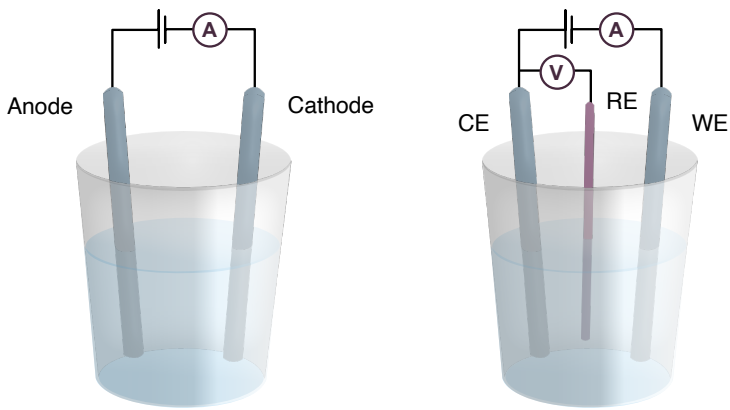

Figure 3.1: A two-electrode cell configuration compared to a three-electrode configuration. The external circuit includes an ammeter (A) and/or a voltmeter (V).

In a three-electrode system, the potential can be measured relative to a specific RE, such as mercury/mercurous sulfate (Hg/Hg_2SO_4) or silver/silver chloride (Ag/AgCl). For consistency and standardization in electrochemical data across different systems, potentials reported in literature are often converted to universal reference scales, such as the standard hydrogen electrode (SHE) or the reversible hydrogen electrode (RHE). In general, SHE and RHE share a similar basic design, however, their primary difference lies in their dependence on the hydrogen ion (H^+) activity in the electrolyte solution. The SHE is defined under standard conditions as the potential of a Pt electrode in an ideal solution, where the H^+ concentration is 1 M at pH 0, and its potential is assigned a value of 0 V. In contrast, the RHE does not have a fixed potential and varies depending on the pH of the solution [56–58].

3.2 Thermodynamic Principles

A simple one-step redox reaction, can be expressed with the following reaction, where an oxidant, O_x, in a solution is reduced to R_{ed} by accepting n number of electrons (e^-) [56]:

$$O_x + ne^- \rightleftharpoons R_{ed} \tag{3.1}$$

The reaction quotient (Q_r) represents the ratio of the activities (a) of the reduced species to the oxidized species. When these activities are close to unity, Q_r can be approximated by the ratio of their respective molar concentrations ([ ]):

$$Q_r = \frac{a_{Red}}{a_{Ox}} = \frac{[R_{ed}]}{[O_x]} \tag{3.2}$$

The Gibbs free energy (ΔG) is defined as the maximum amount of electric work ($-W_{max}$) that can be extracted from a system. It can be expressed as a function of the cell potential (E_{cell}) and the total charge transferred (nF), where F is the Faraday's constant:

$$\Delta G = -W_{max} = -nFE_{cell} \tag{3.3}$$

A redox reaction is spontaneous if $\Delta G < 0$ and non-spontaneous if $\Delta G > 0$. ΔG can be further related to the Gibbs free energy under standard conditions (ΔG^0) and Q_r, where R is the gas constant and T is the absolute temperature:

$$\Delta G = \Delta G^0 + RTlnQ_r \tag{3.4}$$

When $\Delta G = 0$ and the redox reaction is at equilibrium, Eq. 3.3 and 3.4 can be rearranged to yield the Nernst equation for the reaction. In this equation, E^0_{cell} represents the cell potential under standard conditions, corresponding to the theoretical equilibrium cell voltage when no net current flows through the electrodes:

$$E_{cell} = E^0_{cell} - \left(\frac{RT}{nF}\right) lnQ_r \tag{3.5}$$

The Nernst equation can be used to convert potentials between different REs, e.g., the relationship between the potentials of the SHE and RHE can be expressed as:

$$E^0_{RHE} = E^0_{SHE} - \left(\frac{RT}{F}\right) ln10 \cdot pH \tag{3.6}$$

Similarly, the Nernst equation can be applied to other REs, such as Ag/AgCl or $Hg/HgSO_4$. The potential difference between these specific REs and, e.g., the RHE, can be determined using their respective standard electrode potentials (E^0), adjusted with the Nernst equation to account for the activities of the ions involved in the half-reactions. Extensive data on E^0 potentials is available in literature [59].

3.3 Reaction Kinetics

The Nernst equation can provide insight into redox equilibrium states. However, thermodynamics does not determine the rate at which a system reaches equilibrium, as reactions may fail to reach equilibrium, or take varying amounts of time due to kinetic limitations. Understanding and analyzing the reaction kinetics is therefore crucial for a deeper understanding of the electrochemical reactions at play [56].

The rate (r) of an electrochemical reaction is given by the rate constant (k), the concentration of the reactant (C) and the reaction order (α):

$$r = kC^{\alpha} \tag{3.7}$$

The rate constant can be expressed using the Arrhenius equation, which describes its exponential dependence on the absolute temperature:

$$k = Ae^{-\frac{E_a}{RT}} \tag{3.8}$$

Where A is the pre-exponential factor, and E_a is the activation energy.

To drive an electrochemical reaction at a certain rate, an overpotential (η) must be applied to the system, as described by:

$$\eta = E - E_{eq} \tag{3.9}$$

Here, E is the observed potential and E_{eq} is the potential at equilibrium. This overpotential shifts the system away from equilibrium and provides the additional energy required to overcome kinetic or transport barriers, driving the reaction forward.

Chapter 4

Electrochemical Mercury Removal

4.1 Electrochemical Alloy Formation

It is well known that Hg^0 can readily form alloys with various metals, including aluminum (Al), silver (Ag), gold (Au), copper (Cu), tin (Sn), and zinc (Zn), collectively known as amalgams [60]. However, Pt is a notable exception, as its interaction with Hg typically results only in the formation of thin Pt-Hg alloy films [61–64]. Recent studies have demonstrated that electrochemical techniques can facilitate the formation of a stable Pt-Hg alloy, extending beyond thin film formation. Furthermore, this technique has shown significant potential for specific applications in Hg decontamination from aqueous solutions [19–22, 55].

In aqueous solutions, such as natural water, wastewater, and concentrated acid, Hg is commonly present as Hg^{2+} [29]. To effectively decontaminate such solutions, an electrochemical alloy formation technique can be employed. This method involves applying a sufficiently reductive potential to a metal electrode immersed in the solution, inducing the formation of a stable alloy. When Pt is used as the electrode material, alloy phases such as PtHg, $PtHg_2$, and $PtHg_4$ form, with $PtHg_4$ being the most thermodynamically stable and dominant phase [63, 64]. The alloy formation is considered a reversible, multi-step process, with the overall reaction can be expressed as:

$$\mathrm{Pt} + 4\,\mathrm{Hg}^{2+} + 8\,\mathrm{e}^- \rightleftharpoons \mathrm{PtHg_4} \tag{4.1}$$

This process can be described in three main steps, as illustrated in Fig. 4.1: (i) Hg^{2+} are reduced on the surface of the Pt electrode, forming Hg^0. (ii) The Hg^0 interacts with the Pt lattice, integrating into its structure to form the $PtHg_4$ alloy. (iii) Hg^0 atoms diffuse through the $PtHg_4$ layer, enabling continued growth of the alloy [19].

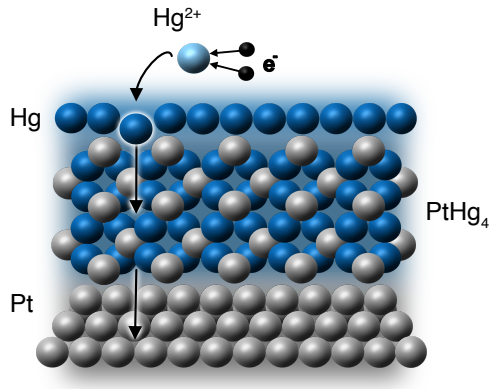

Figure 4.1: The alloy formation process, where Hg^{2+} is reduced on the electrode surface and incorporated into the $PtHg_4$ alloy, followed by diffusion through the alloy and reaction with Pt at the alloy-Pt interface.

In principle, other metals can serve as alternatives to Pt as the electrode material, including Al, Au, Cu, Sn, and Zn. Among these alternatives, Cu is more abundant and cost-effective option compared to Pt. However, its instability in oxidizing acid and water, unless precise potential control is maintained, limits its applicability. In addition, electrochemical regeneration of the Cu-Hg alloy is not viable, as the high positive potential needed to dissolve Hg also oxidizes and dissolves Cu [20]. Au is another potential alternative, as it can from stable amalgam with Hg. However, its higher cost and lower Hg capacity in its most stable form compared to Pt (Au_3Hg vs. $PtHg_4$) make it a less efficient choice [65]. Less noble metals, such as Al, Sn, and Zn also present potential options. However, their high susceptibility to oxidation and degradation under typical operating conditions significantly limits their ability to form stable alloys, making them impractical for most applications [66, 67].

Electrochemical alloy formation as a method for Hg removal offers several important advantages over other current methods, as detailed in Section 2.3. By using Pt as the electrode material, this approach has demonstrated high selectivity for Hg and efficiency across a wide range of initial concentrations of Hg, making it suitable for both industrial and environmental applications. In addition, the process is unaffected by pH in the range of 0 – 6.6, it is relatively energy efficient, and is reversible, allowing for the regeneration of Pt electrodes and safe recovery of Hg. Once the electrodes are saturated with Hg, they can be transferred and regenerated by applying a positive potential in a small volume of solution specifically designed for regeneration. When the concentration of Hg in the regeneration solution reaches a high level, established removal methods, such as precipitation, are expected to recover Hg with high purity [19].

A more in-depth examination is needed to fully understand the exact reaction mechanisms underlying the alloy formation, including detailed thermodynamics, kinetics, and the complexities of the regeneration process. Additional research is necessary to evaluate the method's potential for practical applications, its transition from laboratory scale (lab-scale) to field implementations, and its integration into existing industrial and environmental Hg removal systems.

4.2 Cell Setup

To study electrochemical alloy formation as a method for Hg removal, experiments can be conducted using relatively simple cell setups that involve either a two-electrode or a three-electrode configuration immersed in an aqueous solution containing Hg. In this work, e.g., synthetic solutions are prepared with lab-grade sulfuric acid (H_2SO_4) or nitric acid (HNO_3), in either diluted or concentrated forms. These synthetic solutions are ideal for lab-scale studies as they provide controlled environments for detailed experimentation and analysis. In addition to synthetic solutions, real-world solutions contaminated with Hg, such as industrial wastewater or concentrated acid, are used to investigate the method's potential for practical applications and performance under real-world conditions.

The selection of electrode materials depends on the study's objectives. For fundamental studies at lab-scale, such as investigations into reaction mechanisms, simple Pt electrode designs are often preferred, where e.g., in this work, a thin silica glass plate coated with Pt, provides a well-defined and uniform surface area for controlled experiments. In contrast, studies that require an electrode with high surface area and durability in corrosive conditions, steel or carbon foam-supported Pt electrode can be more suitable [68, 69]. Foam-based electrodes can offer significantly higher surface areas compared to plate designs, enhancing Hg removal rates. This can make foam-based electrodes particularly advantageous for practical applications, where fast and efficient Hg removal is the primary objective. A comparison of the main Pt electrode designs is shown in Fig. 4.2.

Other important components of the cell setup include the CE, which must be carefully selected based on factors such as high conductivity, a sufficiently large surface area to avoid reaction limitations, corrosion resistance, cost-effectiveness, and scalability for practical applications [70]. In addition, in some cases the use of a RE is often impractical or unnecessary. Instead, the cell can be operated in a two-electrode configuration, simplifying the setup, particularly if contamination is a concern at lab-scale, or making it more suitable for scale-up. The cell setup can also include a stirring mechanism or temperature control system. A comparison of a typical lab-scale cell setup and a scaled-up version more suitable for practical applications, both in a batch cell and in a flow reactor system, is shown in Fig. 4.3.

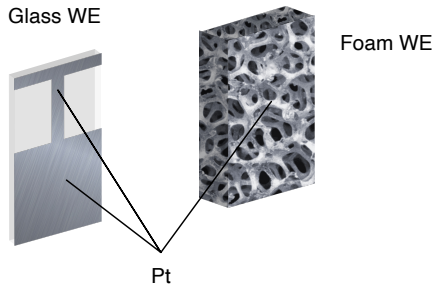

Figure 4.2: A Pt glass plate electrode compared to a steel or carbon foam-supported Pt electrode.

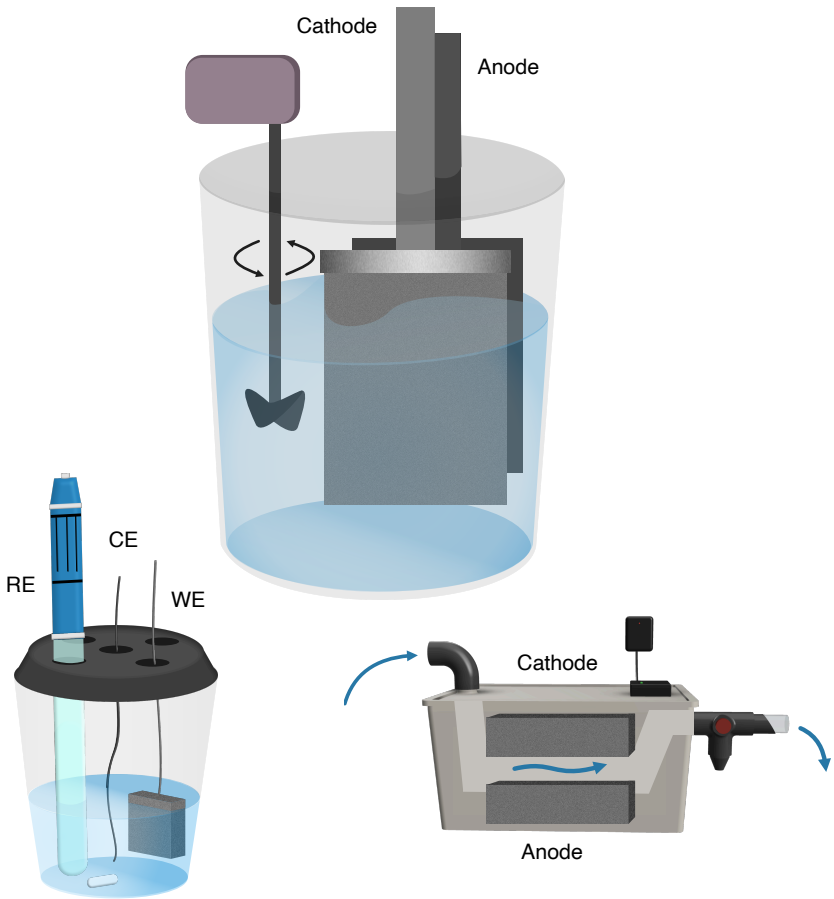

Figure 4.3: An example of a three-electrode setup at lab-scale using Pt glass/foam WE. In addition, a larger-scale reactor with a two-electrode setup utilizing a Pt foam cathode, as well as a flow reactor system.

4.3 Electrochemical Techniques

Dynamic electrochemical methods, which measure potential, current, and/or charge, can provide crucial insights into the complex processes occurring at the electrode-solution interface. A comprehensive understanding of an electrochemical system generally cannot be achieved using one single technique. Instead, multiple complementary methods are often required, each focusing on specific aspects. For electrochemical alloy formation, different dynamic methods can be used to investigate key aspects such as the mechanistic and energetics of the alloy formation process and/or the regeneration of the Pt electrode [56, 59].

4.3.1 Voltammetry

Voltammetry refers to a range of electrochemical techniques used to gather information about an analyte in an electrolyte solution by measuring the current response to a varying potential applied to an electrode. One of the most commonly used methods within voltammetry is cyclic voltammetry (CV). To record a CV, a varying potential is applied to the electrode, and the resulting current is measured as a function of the applied potential. Here, positive currents correspond to anodic processes (oxidation), while negative currents correspond to cathodic processes (reduction). A typical CV is recorded by scanning the potential from an initial value to a set potential and then reversing back to the initial value. The potentials are selected to encompass the electrochemical processes of interest, where the potential scan rate determines the rate at which the applied potential is varied. The resulting CV typically exhibits characteristic peaks corresponding to oxidation and reduction reactions of the analyte and/or electrode material [59].

The electrochemical behavior of Pt has been extensively studied, and its characteristic CV is well-documented [56]. A typical CV of a Pt electrode, as shown in Fig. 4.4, displays key features of Pt electrode in an acidic electrolyte, including: (i) The hydrogen region, representing the adsorption and desorption of hydrogen on the Pt surface. (ii) The double-layer region, where only non-Faradaic (capacitive) currents arise, by changes in the applied potential. (iii) The oxygen region, corresponding to the formation and reduction of Pt oxides at higher potentials.

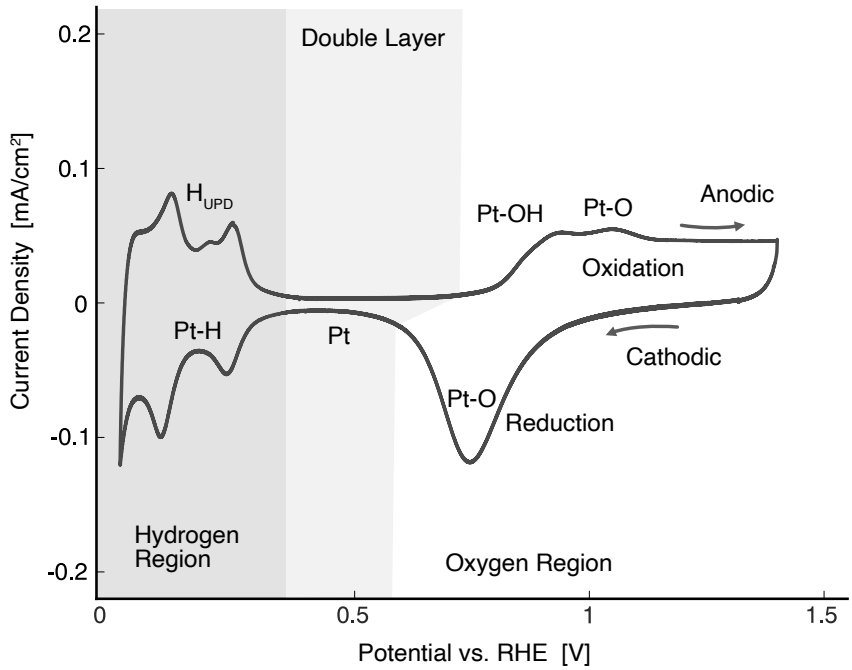

Figure 4.4: A Pt CV recorded in 0.5 M H_2SO_4 at a scan rate of 50 mV/s, showcasing some of its key features [56].

The total charge (Q) associated with specific adsorption/desorption peaks in the CV can be determined by integrating the current (I) under the corresponding peak with respect to the potential, considering the scan rate (dE/dt). Alternatively, expressing the current as a function of time allows integration over the corresponding time range:

$$Q = \int \frac{I}{dE/dt} dE = \int I \, dt \tag{4.2}$$

The electrochemical surface area (ECSA) of the electrode material can be determined from the peaks associated with hydrogen adsorption. In this case, Q is calculated by integrating the area under the hydrogen under-potential deposition (H_{UPD}) peaks:

$$ECSA = \frac{Q}{q\Theta_{max}} \tag{4.3}$$

The determination of ECSA using this approach is based on several key assumptions [71]. It assumes a surface H-coverage of 77 % (Θ_{max}), and considers the surface charge of one monolayer of H adsorbed on polycrystalline Pt to be 210 $\mu C/cm^2$ (q). This value is justified from an equal distribution of the three low-index planes (111), (110) and (100) of Pt.

The roughness factor (RF) of the electrode surface can be determined from the ECSA by dividing it by the geometric surface area (GSA), which can also be considered the projected surface area used:

$$RF = \frac{ECSA}{GSA} \tag{4.4}$$

CV can be a useful tool for studying the electrochemical interactions between a Pt electrode and Hg in solution. It is particularly effective in investigating the reduction and oxidation processes, such as the formation and dissolution of the $PtHg_4$ alloy. Understanding the characteristic behavior of a Pt CV in the absence of Hg is crucial for identifying deviations when Hg is introduced into the electrolyte solution. Such deviations can include appearance of new features, shifts in specific regions, or suppression of peaks.

4.3.2 Electrochemical Quartz Crystal Microbalance

Electrochemical quartz crystal microbalance (EQCM) is a technique that combines the principles of electrochemistry and piezoelectricity to investigate in real-time various electrochemical processes [72, 73]. In particular, EQCM can precisely measure mass changes in thin films on an electrode during processes such as electrodeposition and dissolution of metal films. By using EQCM, kinetic examination of processes that involve events at the monolayer level and thin films are able to be examined [74].

The operation of an EQCM relies on a quartz crystal sensor coated with electrodes on both sides. When an alternating electric field is applied, the crystal oscillates at a specific resonant frequency (Δf_0). This frequency of oscillation is highly sensitive to the mass of the crystal, meaning that any addition or removal of mass on its surface causes shift in frequency [72]. The EQCM can be combined with a technique called dissipation monitoring (EQCM-D), in which both frequency and dissipation changes are recorded simultaneously. Dissipation, defined as the total energy lost in the system per oscillation cycle, can provide additional insights beyond standard EQCM, such as the viscoelastic properties of the films forming on the surface [72, 75].

The Sauerbrey equation can be used to relate the frequency shifts of the crystal to the mass change:

$$\Delta f_n = -\frac{2f_0^2 n}{A_s\sqrt{\rho_q \mu_q}}\Delta m \tag{4.5}$$

Where f_0 is the resonant frequency of the the sensor before any mass change, n is the overtone, A_s is the active surface area of the electrode, μ_q is the shear elastic modulus and ρ_q is the density of quartz [76]:

For the Sauerbrey equation to be valid, certain conditions must be met. The deposited or removed film on the surface must be rigid, contribute to less than 2% of the total mass of the crystal sensor, and be uniformly distributed across its surface. A film can be considered rigid if the frequency shifts of different overtones overlap and the dissipation changes (ΔD) are minimal, and approaching zero. Any deviations from these conditions can result in inaccuracies in the calculated mass changes [72, 77].

ΔD can be expresses as the sum of all energy losses in the system (Q_s) per oscillation cycle. The Q_s factor can be further defined as the ratio of f_0 to the resonance peak bandwidth (BW):

$$\Delta D = \frac{1}{Q_s} = \frac{BW}{f_0} \tag{4.6}$$

EQCM-D can be used for real-time analysis of the electrochemical alloy formation process, including the formation and dissolution of the Hg alloy and the regeneration of the Pt electrode. A typical Pt electrode for EQCM-D is shown in Fig. 4.5. The electrode consists of a planar AT-cut quartz crystal sensor mounted in a dip holder, with only the top Pt electrode exposed to the electrolyte solution.

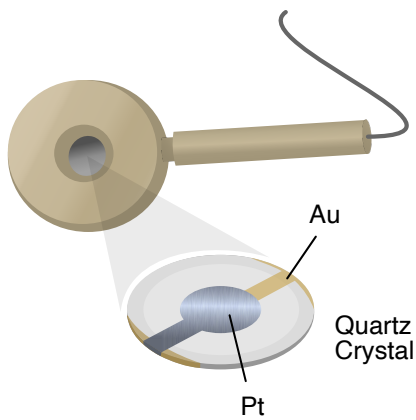

Figure 4.5: EQCM quartz crystal sensor, which can be mounted inside a dip holder.

4.4 Analytical Techniques

In electrochemical research, the ability to identify, quantify, and study the properties of materials and metals of interest is crucial. For certain Hg removal studies, monitoring the concentration of Hg in the solution during electrochemical treatment often involves periodic sampling. These samples are analyzed using certified techniques for accurate Hg quantification in solution. Alternatively, techniques, such as CV and EQCM, provide real-time monitoring of the electrochemical processes without requiring additional sampling, except in specific cases where complementary data might be needed. Physical characterization techniques further provide detailed insights into the structure, composition, and surface property changes of the $PtHg_4$ alloy [56].

4.4.1 Hg Quantification

Inductively Coupled Plasma Mass Spectrometry

Inductively coupled plasma mass spectrometry (ICP-MS) is a widely used technique for measuring trace and ultratrace levels of elements in various matrices, including aqueous solutions. ICP-MS has diverse applications, particularly in fields such as environmental and pharmaceutical monitoring, clinical research, and toxicological studies. Recently, there has been a significant shift towards the use of ICP-MS in clinical labs, owing to the many advantages it can offer over other common techniques, such as atomic absorption (AAS). The main advantages of ICP-MS include multi-element detection, low detection limits, and high sample throughput. However, the initial cost of ICP-MS instrument can be high, as well as the operating costs themselves, as the system requires argon gas and other high purity gases. Nonetheless, the advantages of the ICP-MS often outweigh these expenses, particularly in settings where precise and accurate trace element analysis is essential [78, 79].

The operation of an ICP-MS instrument can be described in four main steps: (i) The sample, typically an acidic solution, is introduced into the system via a peristaltic pump and is nebulized into a fine aerosol. (ii) This aerosol is transported into a plasma torch, where the sample is atomized and subsequently ionized. (iii) The ions generated in the plasma are extracted and guided into a mass analyzer through a set of electrostatic lenses or ion optics. (iv) In the mass analyzer, the ions are separated based on their mass-charge (m/z) ratios and the abundance of different isotopes are measured in the detector, which allows for the quantification of the elements present in the original sample [78].

When using ICP-MS for Hg quantification, several factors must be considered. Hg is a volatile element and is notorious for its memory effect, in which a prolonged signal persists long after the initial sample has been analyzed, even after an appropriate washout time has been carried out [80–82]. This effect can lead to a non-linear calibration of the instrument, reduced sensitivity over time, and a high dependency of the signal on the sample matrix. Even at low Hg concentrations the memory effect can be significant, as Hg can adhere to

the walls of both the ICP-MS transfer tube and the spray chamber. Several steps have been proposed to mitigate the memory effect of Hg, including the addition of Au and stabilizing agents to the sample, as well as specific acid rinsing solutions [83, 84].

In the context of Hg removal via electrochemical alloy formation, ICP-MS can be used to quantify Hg and other metals of interest in solution, such as Pt and iron (Fe). To stabilize against Hg^{2+} reduction during analysis, 1 M hydrochloric acid (HCl) is used to prepare the samples [84]. In addition, calibration standards are carefully prepared to exactly mirror the sample matrices from the electrochemical measurements. Internal standards can be added to all samples to further correct for random errors, such as noise, torch instabilities, and matrix effects. These internal standards are selected based on their atomic mass and ionization potential, which are similar to those of the element of interest, allowing for instrumental fluctuations to be accounted for [85]. By implementing these measures, the memory effect during Hg analysis with ICP-MS can be minimized, leading to negligible deviations and eliminating the need for further preventative steps to ensure precise and reliable results.

Atomic Absorption Spectroscopy

AAS is an analytical technique used to measure trace and ultratrace levels of elements in various sample matrices, including aqueous solutions. It is widely applied in fields such as environmental monitoring, food safety, and clinical diagnostics. In AAS, the absorption of light by free gaseous atoms is measured. These atoms absorb light at characteristic wavelengths corresponding to the emission lines of the element being analyzed. The difference in light intensity, measured before and after atomization, is proportional to the concentration of the element in the sample [79]. AAS can exist in various forms, such as flame AAS (FAAS), graphite furnace AAS (GFAAS), vapor generation AAS (VAAS), and cold vapor AAS (CVAAS), each tailored for specific applications. Among these, CVAAS is specifically designed for Hg analysis, as other AAS techniques can often lack the required sensitivity [79]. However, as an alternative to conventional CVAAS, the Direct Mercury Analyzer (DMA) has emerged as a particularly effective AAS-based method for Hg detection [86].

In a DMA instrument, samples are first prepared by weighing them into quartz or metal sample trays, which are then placed in the instrument's autosampler. The analysis process can be described in five main steps: (i) The samples are dried and thermally decomposed in a furnace under an oxygen atmosphere, releasing Hg from the sample matrix. (ii) The released Hg passes through a catalyst section in the furnace, where interfering compounds and byproducts that could affect the accuracy of the measurement are removed. (iii) Hg is captured on a Au amalgamation trap, where it is concentrated while combustion byproducts are flushed out. (iv) The amalgamation furnace is heated to release the trapped Hg. (v) Hg is then carried by a flow of inert gas into a specialized system, where the Hg concentration is determined using AAS [86].

In the context of Hg removal via electrochemical alloy formation, DMA can be used to quantify Hg in solution. Unlike other analytical techniques, such as ICP-MS, DMA does not require special procedures to mitigate Hg memory effects. Furthermore, it does not involve any other sample pre-treatment or the addition of chemicals. Despite its simple operation, DMA can achieve a detection limit as low as 0.0015 ng [86]. However, a notable limitation is that DMA is selective only for Hg and cannot detect other elements such as Pt, Cu, or Fe.

4.4.2 Electrode Material Characterization

Scanning Electron Microscopy

Scanning electron microscopy (SEM) is a versatile technique used to analyze surfaces of materials. It is widely used across various fields, including nanotechnology, archaeology, medical devices, and forensic science. Its operation involves irradiating a sample with a high-energy electron beam, typically up to 30 keV. The electrons interact with the atoms in the sample, producing a variety of signals, such as secondary electrons (SE) and backscattered electrons (BSE), originating from different interactions and depths within the sample's volume. SEs are low-energy electrons (< 50 eV), ejected from the outer orbitals of atoms due to inelastic scattering. Because of their low energy, SE signals are generated from a shallow depth, typically a few nanometers below the surface, where the signal strength depends on factors such as the angle of incidence of the electron beam. BSEs are high-energy electrons from the incident beam that are elastically scattered by the sample's atoms, where heavier elements scatter electrons more effectively than lighter elements, providing contrast based on atomic number [87].

SEM can be a valuable tool to investigate the $PtHg_4$ alloy formed on the electrode after electrochemical alloy formation. SEM can provide detailed insights into the surface topography, revealing features such as surface roughness and morphological changes relative to the electrode's initial state before any electrochemical treatment.

X-Ray Diffraction

X-ray diffraction (XRD) is a technique used to study structural and compositional properties of crystalline materials. It is widely applied across various fields, including the pharmaceuticals industry, geological applications, and forensic science. XRD involves directing a beam of X-rays at a crystalline material, which scatters the X-rays in various directions. The constructive interference of these scattered X-rays produce a diffraction pattern unique to the materials structure [88].

XRD can be used to characterize the $PtHg_4$ formed on the electrode during electrochemical alloy formation. By analyzing its distinct diffraction patterns, specifically the angles and intensities of the diffracted beams, XRD can provide insights into the alloy's crystalline structure, elemental composition, and predominant phase.

Chapter 5

Advancing Electrochemical Alloy Formation

5.1 Fundamental Investigations

To advance electrochemical alloy formation as a Hg removal method, it is essential to gain a comprehensive understanding of how the Pt electrode interacts with Hg in solution. Key aspects to investigate include, but are not limit to, the reaction mechanisms underlying the alloy formation, the associated energetics and kinetics parameters, and processes involved in the alloy oxidation and Pt electrode regeneration.

5.1.1 Alloy Formation

Interactions Between Platinum and Hg

To investigate the detailed electrochemical interactions during alloy formation between the Pt electrode and Hg ions in solution, CV studies were conducted, and described in **Paper II**. The recorded CVs, are shown in Fig. 5.1. A clear difference in the recorded CVs is observed when Hg is present in the solution compared to a typical Pt CV in the absence of Hg, as shown in Fig. 5.1a. In the Hg solution, the H^+ adsorption/desorption peaks are significantly suppressed due to the interaction of Hg ions with the electrode surface and the formation of a Pt-Hg alloy. In addition, the oxidation peak, representing a combination of Hg oxidation/dissolution and Pt surface oxidation, shifts to higher potentials and becomes substantially larger compared to the Pt CV recorded without Hg. Notably, this new oxidation peak is consistently observed at the same potential (1.2 V vs. SHE), regardless of the duration of the applied potential and the alloy formation process, as shown in Fig. 5.1b–f.

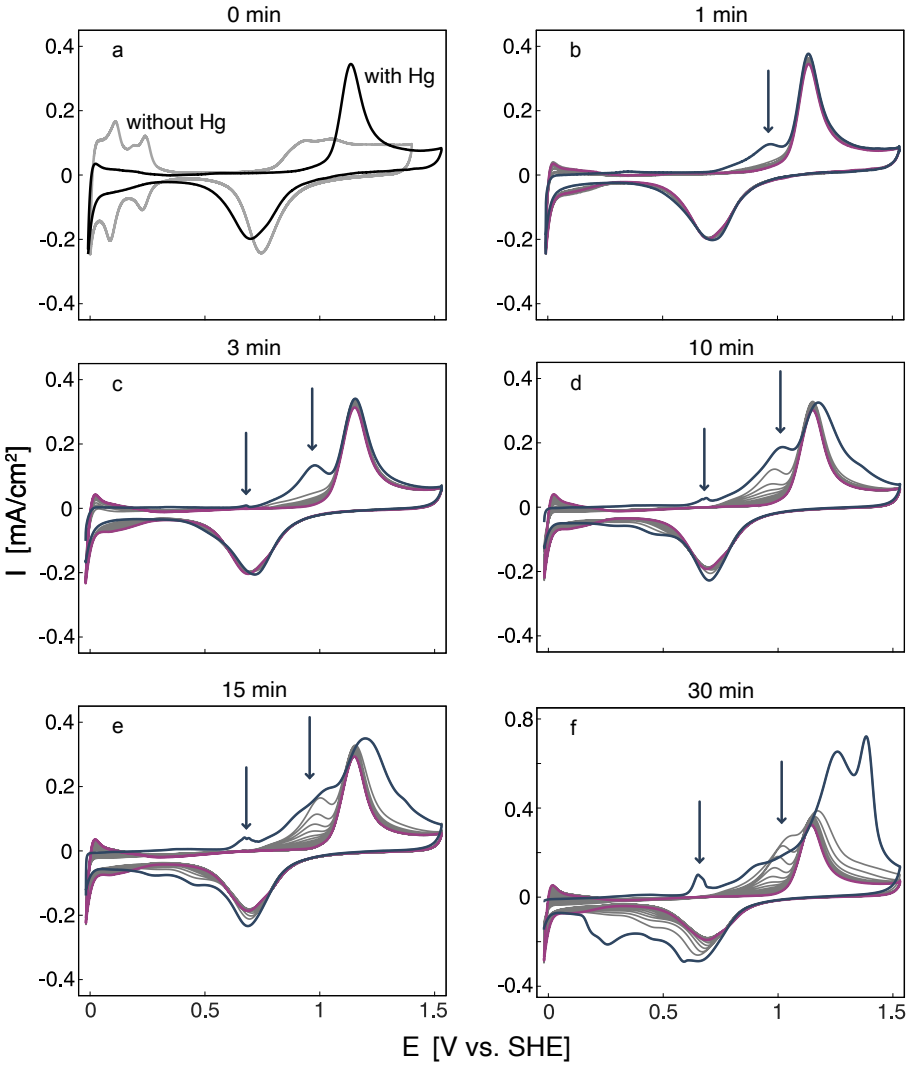

Figure 5.1: (a) CV of Pt in 0.5 M H_2SO_4 at a scan rate of 50 mV/s, with 10 mg Hg/L (black) and without Hg (gray). (b–f) CVs with 10 mg Hg/L, after potential holds at 0.18 V vs. SHE for 1 – 30 minutes. The dark blue represents the initial CV cycle immediately following the potential hold, the gray represent the intermediate CV cycles, and the magenta corresponds to the final CV cycle.

The $PtHg_4$ alloy formed on the electrode continues to grow with longer potential holds and alloy formation, as evidenced by increasing peak associated with the oxidation of $PtHg_4$ at approximately 1.2 V vs. SHE. In addition, Hg^0 forms on the surface, indicated by another peak at 0.6 – 0.7 V vs. SHE, which continues to increase during longer potential holds. The oxidation of the multilayer $PtHg_4$ alloy requires multiple cycles to fully return to its baseline, whereas Hg^0 is removed from the surface during the first anodic scan following each potential hold.

To further investigate the dependence of alloy formation on applied potential, EQCM-D was used and discussed in **Paper II**. When a slow potential scan is applied, transitioning from conditions where no alloy forms to those sufficiently reductive to induce its formation (0.80 – 0.18 V vs. SHE), the alloy exhibits linear growth over time. In addition, the EQCM-D studies suggest that Hg^0 forms on the Pt electrode surface during alloy formation, aligning with the observations from the CV studies. After alloy formation, applying a constant potential of 0.80 V vs. SHE initially causes a decrease in mass detected on the surface, followed by its stabilization at the same potential, indicating effective removal of Hg^0 from the electrode surface. Furthermore, this slow potential scan reveals the onset potential for the alloy formation as 0.64 V. This onset potential closely aligns with DFT calculations presented in **Paper II**, which predict the theoretical reversible potential for this system to be 0.78 V vs. SHE, from a thermodynamic standpoint. Given the onset potential of 0.64 V vs. SHE, the process thus exhibits an overpotential of around 0.14 V, indicating that additional energy is required to drive the alloy formation reaction beyond its thermodynamic limit. It is important to note that in this case, the alloy formation process has low Faradaic efficiency. The currents associated with Hg deposition are extremely low due to the low concentrations of Hg in the electrolyte. During Hg deposition, the measured current during deposition is dominated by the oxygen reduction reaction (ORR) from dissolved O_2. An estimation of the maximum current generated from Hg^{2+} reduction, assuming a diffusion layer of 100 μm, ranges from approximately 2 – 20 $\mu A/cm^2$ for a solution containing 1 – 10 mg/L of Hg. Similarly, for a concentration range of 10 – 100 μg/L, the estimated current would be 20 – 200 nA/cm^2. As a results, current measurements are very difficult to use to estimate Hg deposition, instead, the mass change recorded by EQCM-D was used to determine onset potential and amount of Hg adsorbed.

As demonstrated by the CV studies, the duration of the potential hold and alloy formation results in a corresponding increase in the total charge stripped from the electrode's surface. This charge, attributed to Hg oxidation, is quantified for potential ranges corresponding to the electrochemical reactions of both Hg^0 and the $PtHg_4$ alloy. The charge can be directly correlated to the mass of Hg per unit area of the electrode, assuming that all stripping charge arises from Hg oxidation and all Hg is oxidized to Hg^{2+}. The relationship between the mass of Hg and potential hold duration, for both the total accumulated Hg and only Hg^0, is shown in Fig. 5.2. A clear linear relationship is observed, indicating that the rate of Hg addition on the electrode remains constant over

time, consistent with the findings in **Paper I**. In **Paper I**, the alloy formation was studied over a significantly longer time using EQCM-D, where the mass change was monitored for over 40 hours, compared to a maximum duration of 30 minutes in the CV studies in **Paper II**. The results, shown in Fig. 5.3, further indicate that the alloy formation remains constant over time and is not affected by the growing alloy film.

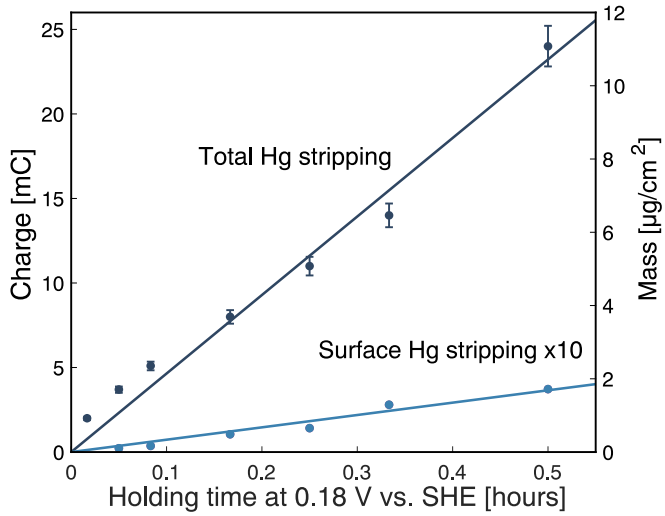

Figure 5.2: Net positive charge associated with Hg oxidation as a function of time. The light-blue line is scaled by a factor of 10 for visibility.

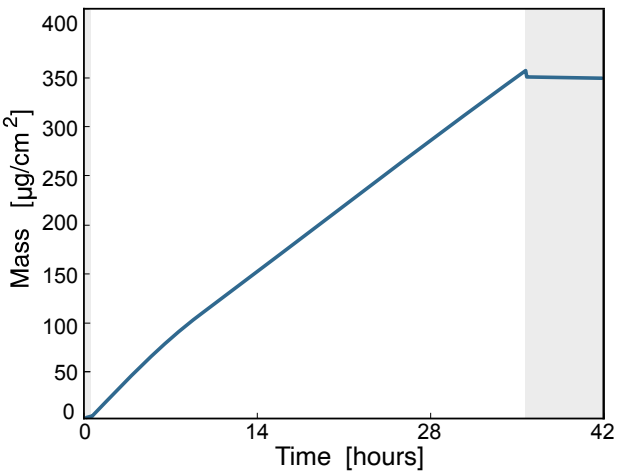

Figure 5.3: Mass change as a function of time recorded with EQCM-D in 0.5 M H_2SO_4 with 10 mg Hg/L. 0.18 V vs. RHE was applied in the white region.

Influence of Concentration and Temperature on Hg Removal

Paper I describes how the efficiency of Hg removal and alloy formation process is strongly influenced by the initial Hg concentration in the solution. More specifically, at lower Hg initial concentrations, the Hg content decreases at a higher rate compared to higher concentrations, as shown in Fig. 5.4, for an initial Hg concentration range of 0.25 – 1000 μg/L. This difference is likely due to variations in the Pt:Hg ratio in the solution. At lower concentrations (0.25 – 10 μg/L), a full monolayer of the alloy never forms, as there is insufficient Hg available in the solution. In contrast, at higher concentrations (1000 μg/L), a full monolayer develops within approximately 0.5 hours. When no monolayer of alloy is present, alloy formation occurs directly at the Pt surface. Once fully formed, Hg diffuses through the alloy layer to interact with Pt at the Pt-alloy interface.

Based on the general rate expression for alloy formation, outlined in **Paper I**, the apparent reaction order for Hg^{2+} concentration is approximately 0.8. This reaction order, of less than 1, suggests that the alloy formation process does not directly proceed via Hg^{2+} in the solution. Instead, it is more likely that the reaction proceeds through the formation of Hg^0 on the surface and followed by the alloy formation. If the plating of Hg^0 occurs faster than the alloy formation, Hg^0 can accumulate on the surface, resulting in this apparent reaction order of less than 1.

The relationship between the alloy formation and temperature was investigated in **Paper I**. It is clear that the rate of Hg removal increases with temperature, and follows an Arrhenius behavior. By constructing an Arrhenius plot, the apparent activation energy for the overall reaction of $PtHg_4$ is determined to be 0.29 eV. This relatively low value indicates a low threshold energy for the reaction to occur. Similarly, in **Paper II**, the overpotential for alloy formation process is also a measure of a barrier that the reaction must overcome to proceed.

For the electrochemical Hg removal method to be applicable across different environmental and industrial settings, its effectiveness must be demonstrated across a broad concentration range. This includes scenarios where the target Hg concentration is often well below the WHO limit of 6 μg/L, as well as industrial cases where solutions can contain significantly higher Hg concentrations. In **Paper I**, the Hg removal method demonstrated its effectiveness across a wide range of initial Hg concentrations, as shown in Fig. 5.4. The Hg content is reduced in all cases to levels well below the drinking water limit set by WHO (6 μg/L) within 30 hours, starting from initial Hg concentration ranging from 0.25 – 1000 μg/L. Furthermore, successful Hg removal was demonstrated in a solution with extremely high initial Hg concentration of 75,000 μg/L. It is important to note that due to the current measurement procedures and detection limits of the ICP-MS used, studies with initial Hg concentrations lower than 0.25 μg/L could not be conducted. However, it can be expected that the electrochemical alloy formation method can also effectively remove Hg from solutions at substantially lower concentrations.

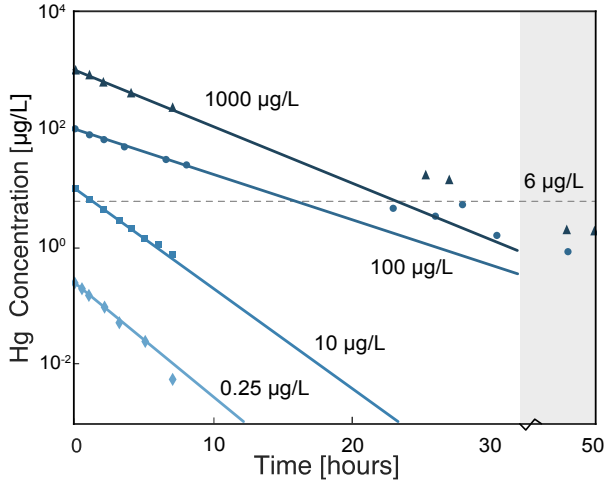

Figure 5.4: Hg concentration as a function of time, for different initial concentrations. The dashed line corresponds to the WHO guideline for safe drinking water (6 µg/L).

Regeneration

Effective regeneration of the Pt electrode after electrochemical treatment is essential for both the recovery of Hg from the solution for disposal and for enabling the reuse of the electrode. This is particularly important considering that Pt is an expensive and scarce metal. From an economic perspective, the regeneration process should ideally be completed as quickly and efficiently as possible. However, applying excessively high potential can lead to unwanted side reactions and potential degradation of the electrode material. Therefore, identifying the optimal regeneration potential window, one that is neither too low to hinder the process nor too high to cause damage, is crucial.

As one of the first steps in studying the regeneration process, EQCM-D analysis, as presented in **Paper II**, was used to determine the onset potential for the dissolution and oxidation of the $PtHg_4$ alloy, which was found to be 0.98 V vs. SHE. This was conducted similarly to the method used in the previous section to determine the onset potential for alloy formation. In addition, DFT calculations, which yield reversible potential of 0.78 V vs. SHE, indicate that the alloy oxidation occurs with an overpotential of approximately 0.2 V. Notably, the overpotential is relatively symmetric, with values of approximately 0.14 V for alloy formation and 0.2 V for oxidation.

Applying current instead of potential can offer significant advantages for the regeneration process, particularly when adapting it to practical applications, as constant current can be easier to implement. When using constant potential, small variations in the cell setup, such as electrode condition or solution resistance, can result in significant fluctuations in current. A constant current approach can maintain a more stable system, improving the overall performance of the regeneration process. By controlling the current, the rate of the reaction can be more precisely controlled. In contrast, when controlling the potential, there is a risk of setting it just below the threshold required to drive the reaction, resulting in no reaction at all. Setting the potential slightly too high can result in an excessively high reaction rate.

In addition to the EQCM-D regeneration studies using potential, further EQCM-D studies were carried out at a constant current of 5 μA, in a same cell as shown in **Paper II**. A graphite cathode was used to prevent the plating of released Hg from the Pt electrode onto the cathode. Five consecutive cycles of alloy formation and regeneration were performed, with approximately 16.5 $\mu g/cm^2$ of Hg absorbed on the Pt electrode during each alloy formation step, representing the amount Hg removed from the solution. The Hg removal process was carried out for around 45 minutes, while the regeneration process was completed in just a few minutes. The regeneration percentage, representing the relative amount of Hg removed and released in each cycle is shown in Fig. 5.5. The regeneration efficiency for all five cycles is more than 95%. Importantly, the Pt electrode demonstrates stability and efficiency throughout the five cycles of continuous Hg removal and regeneration.

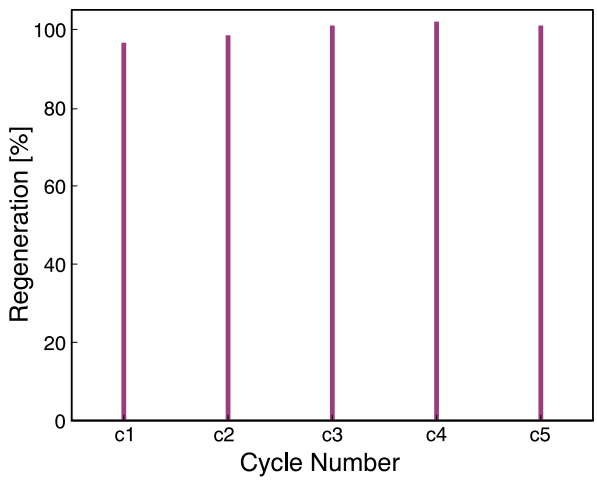

Figure 5.5: The regeneration percentage of five cycles of alloy formation and regeneration at a constant current of 5 μA.

To study the regeneration of a Pt electrode for practical applications, a Pt carbon foam electrode was used instead of the EQCM Pt electrode. The foam electrode and a similar Hg removal process at lab-scale are described in **Paper III**. The foam electrode was regenerated using the same method as for the EQCM electrode, achieving a regeneration efficiency of approximately 80%. During the initial Hg removal, 0.33 mg/kg of Hg was removed from concentrated H_2SO_4, while 0.27 mg/kg was released back into a 0.5 M H_2SO_4 regeneration solution.

5.2 Practical Applications

To transition electrochemical alloy formation from a lab-based Hg removal method to a practical and viable solution for Hg removal from aqueous solutions, it is crucial to evaluate its applicability in real-world scenarios. The method must be capable of operating in diverse and complex environments, including natural water and industrial wastewater with varying Hg concentrations and compositions, as well as the highly corrosive conditions found in concentrated acid.

5.2.1 Wastewater from Dental Clinics

Wastewater from dental clinics is a frequently overlooked source of Hg pollution. For over 150 years, Hg has been a key component in dental amalgams, which consist of Hg and at least one other metal [89]. Its exact Hg content is determined by the manufacturer, typically around 50% Hg, with the remainder composed of metals such as Ag, Au, Cu, Tn, and Zn [67, 90]. While the use of dental amalgam has been banned or is being phased out in many regions, it remains widely used in others [91, 92]. As a result, amalgam waste continues to be a significant global concern. Even in regions where bans are in place, it remains an issue, as many patients still have amalgam fillings placed before the regulations were implemented [90].

Hg waste is generated during dental procedures, particularly when amalgam fillings are removed or replaced, allowing Hg to enter wastewater systems and ultimately reach public sewer systems and the environment [93, 94]. In 2013, it was estimated that more than 300 tonnes of Hg were used annually in dental amalgams, with approximately 100 tonnes entering wastewater from dental clinics each year [37]. In 2018, Hg emissions from Swedish dental clinics into outgoing wastewater were estimated to range from 0.1 – 56 g of Hg per dental chair annually, corresponding to total emissions of 1 – 500 kg of Hg released into the environment [90].

Current Hg decontamination methods for wastewater from dental clinics primarily rely on dental amalgam separators, which capture large fragments and particles of dental amalgams, through sedimentation, filtration, or centrifugation [95, 96]. However, these separators have notable limitations, as studies have shown that significant amounts of Hg can still remain in the wastewater even after treatment [90, 95, 97, 98]. Therefore, more efficient and targeted Hg removal technologies are needed to address the challenges associated with Hg contamination in wastewater from dental clinics.

Mercury Removal

To evaluate the feasibility of using electrochemical alloy formation for removing Hg from dental wastewater, lab-scale studies were conducted using real wastewater sourced from a dental clinic, as presented in **Paper IV**. The results, shown in Fig. 5.6, demonstrate that over 85% of the total Hg content was successfully removed within 150 hours.

Building on the positive results obtained at lab-scale, Atium AB developed a commercial flow reactor system based on electrochemical alloy formation and installed it at dental clinics as an additional Hg removal step following existing amalgam separators. The flow reactors operated continuously for up to 440 days, with Hg removal per clinic ranging 20 – 440 mg per cathode, as shown in Fig. 5.7. Each reactor contained 17 cathodes, and at designated intervals, a single cathode was extracted and analyzed for Hg content. Assuming homogeneous Hg uptake across all cathodes, the total Hg removal per reactor was estimated to range from around 340 – 7480 mg, while treating 25,000 L of wastewater. This variation in Hg removal among clinics was influenced by factors such as the size of the clinic, the piping systems in place, and the demographics of the patients.

The results confirm that amalgam separators alone are insufficient to fully capture the Hg present in dental wastewater, highlighting the need for additional Hg removal measures. Incorporating additional treatment steps, such as the flow reactor system, presents a promising solution for dental clinics to reduce the release of Hg into local water systems. Further development of the electrochemical method and the flow reactor for dental clinics, as well as other types of wastewater, could facilitate its integration into broader waste management systems where Hg contamination is a concern.

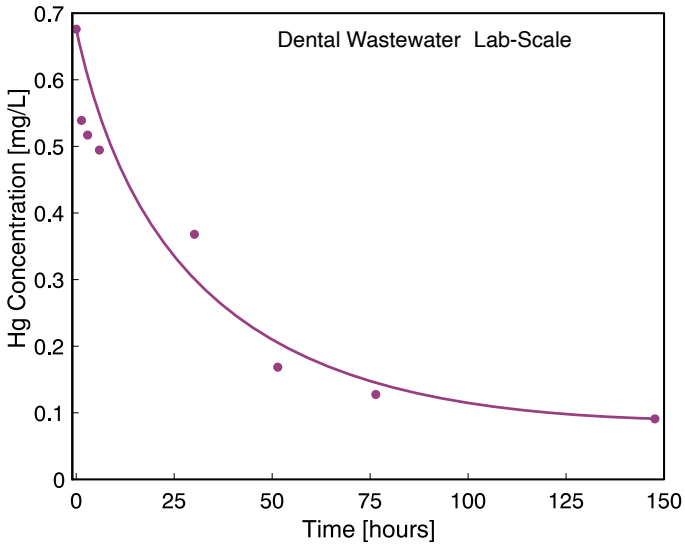

Figure 5.6: Hg removal in dental wastewater using electrochemical alloy formation.

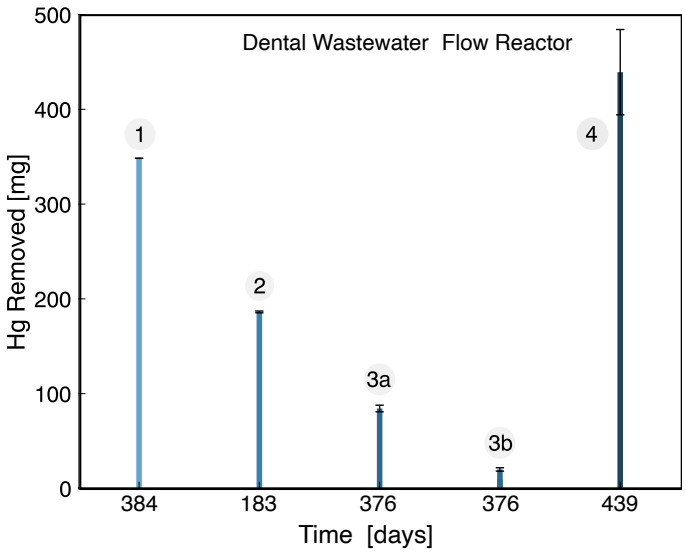

Figure 5.7: Amount of Hg removed in four dental clinics, with clinic numbers indicated in gray. Two reactors are installed at the third clinic (3a and 3b).

Figure 5.8: Photograph of the commercial flow reactor system installed at a dental clinic, positioned downstream of the amalgam separator and upstream of the sewer outlet.

5.2.2 Concentrated Sulfuric Acid from Smelting Plants

Concentrated H_2SO_4 (93–98 %) is one of the most widely used chemicals in the world today, with an annual production of more than 200 million tonnes. It has a wide range of applications, including in fertilizer production and the paper industry [99, 100]. When H_2SO_4 is produced from zinc and copper smelting processes, it can be highly contaminated with Hg, as the ore itself can contain varying amounts of Hg [101]. During the smelting process, Hg in the ore is volatilize as Hg vapor, exits with the off-gases and enters the H_2SO_4 product [25, 102]. Although gas-phase cleaning methods can mitigate some of the Hg contamination, these technologies are expensive and often inadequate for reducing Hg levels to meet stringent regulatory limits [103]. For commercial applications, H_2SO_4 is typically classified into two quality grades based on its Hg content, where it is considered technical-quality when its Hg content is below 0.30 mg/kg and high-purity grade when Hg is below 0.08 mg/kg [101]. The acceptable level of Hg contamination in H_2SO_4 often depends on its intended application, as the acid is used across various industries and can contribute to Hg contamination in both end products and wastewater. This can lead to Hg entering the environment, posing risks to ecosystems and increasing the potential for human exposure [102]. The issue of Hg contamination in concentrated H_2SO_4 is therefore a significant concern, in particular as no commercial solution currently exists for effectively removing Hg from concentrated acids [16].

Hg Removal

In **Paper III** it is reported for the first time that Hg can be removed from concentrated H_2SO_4 acid. The study demonstrates that using electrochemical alloy formation as a Hg removal method, over 90% of the Hg content was removed from the acid at lab-scale within 120 hours, where technical-grade quality is achieved in 20 hours, and high purity within 80 hours. To evaluate the scalability of the method for potential industrial-scale decontamination, the method was scaled up 400-fold, from a 50 mL lab-scale cell setup to a 20 L reactor, as shown in Fig. 5.9. Photographs of the reactor are shown in Fig. 5.10. In the reactor, over 98% of the Hg content was removed within 160 hours, achieving technical-grade quality after 20 hours and high purity within 80 hours.

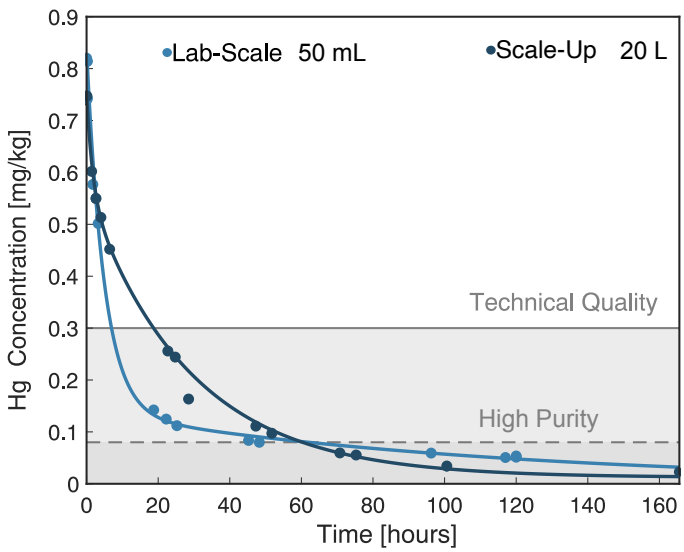

Figure 5.9: Hg removal from concentrated H_2SO_4, both at lab-scale (50 mL) and scale-up (20 L), using electrochemical alloy formation.

Electrochemical alloy formation as method for Hg removal shows significant potential for treating concentrated acids at an industrial-scale, where hundreds or even thousands of tonnes of concentrated H_2SO_4 must be processed to meet Hg commercial limits and time constraints. However, treating concentrated acid presents a substantial engineering challenge, particularly in identifying suitable materials. The Pt electrode material must withstand high corrosion and possess a high surface area to enhance the rate of Hg removal while minimizing the amount of Pt required. Stainless Steel 316L (SS316L), commonly used in industrial storage and handling of concentrated H_2SO_4, was employed as the substrate for the Pt electrode in the form of foam [68, 104].

However, during the removal process, the SS316L foam electrode exhibited poor corrosion resistance, resulting in Fe leaching above acceptable technical limits, and thus it is unsuitable for future applications. To prevent potential Fe contamination of the acid, a metal-free candidate, such as a reticulated vitreous carbon (RVC) foam can be used as an alternative to SS316L foam. As shown in **Paper III**, RVC demonstrated excellent stability in concentrated H_2SO_4, and efficient Hg removal. Around 90% of the Hg content was removed at lab-scale with levels reduced below technical grade and down to 0.10 mg/kg, which is just above the high-purity limit. The RVC, or other carbon-type foams, appear to be highly promising candidates for the Pt electrode in the development of this method, with the goal of achieving industrial-scale decontamination of the concentrated acid.

Figure 5.10: Photographs of the scale-up (20 L), showing the reactor setup and a SS316L Pt foam electrode.

Chapter 6

Conclusion

Hg pollution in water is a global environmental and public health concern, with lasting implications for both current and future generations. Its persistence and continuous cycling through the environment make Hg pollution a long-term challenge that needs an effective intervention. Existing methods for Hg removal have notable limitations, particularly the ones used to treat aqueous solutions such as natural water, wastewater, and industrial effluents. Therefore, developing new and more efficient removal methods is essential. In this context, electrochemical alloy formation has emerged as a promising technique for Hg removal, effectively addressing some key limitations of current removal methods.

The research presented in this thesis aims to provide valuable insights into electrochemical alloy formation as an effective method for Hg removal from aqueous solutions. For successful implementation under practical conditions, it is crucial to establish a fundamental understanding of the electrochemical processes involved in this removal technique. By combining electrochemical and analytical techniques, the interactions between Hg ions in solution and the Pt electrode are studied in detail, with a focus on the thermodynamic and kinetic parameters governing alloy formation and its dissolution (oxidation). A series of studies demonstrate effective Hg removal from solutions across a wide range of initial Hg concentrations, from low levels relevant to environmental applications, such as in natural water, to high concentrations representative of industrial processes dealing with severe Hg contamination. In addition, the influence of temperature on alloy formation is examined, as understanding this relationship is crucial due to significant temperature variations that can exist in different industrial streams.

To explore the method for practical applications, a flow reactor system based on the electrochemical method was successfully used to capture significant amounts of Hg from wastewater at dental clinics. This flow reactor removed Hg that was not captured by the existing removal methods in place. Without such intervention, this Hg would be released into the environment through the wastewater. In another practical application, Hg was successfully removed from concentrated H_2SO_4, by using electrochemical alloy formation, not before

reported by other established removal methods. Hg was effectively removed from the concentrated acid derived from a zinc smelter, resulting in high-purity acid with Hg content below key industrial limits. The method was subsequently scaled up 400-fold, from lab-scale to a medium-sized demonstration system, maintaining efficient Hg removal and demonstrating excellent scalability. These results highlight the method's potential for industrial-scale decontamination of concentrated acid, where Hg contamination is a persistent challenge and difficult to mitigate with conventional techniques.

Outlook

Electrochemical alloy formation holds great potential as a method for Hg removal, however, there are challenges and limitations to consider. To develop this technique into a viable decontamination method for practical applications, every stage of the Hg removal process must be thoroughly designed and optimized. Establishing a comprehensive end-to-end Hg removal method requires careful consideration of all steps: (i) Hg removal and alloy formation, (ii) alloy dissolution and electrode regeneration, and (iii) the safe recovery and disposal of Hg.

In this thesis, significantly more studies have been conducted on the alloy formation process than on the regeneration process. However, electrode regeneration is equally important for developing a fully functional removal method. Future research should focus on optimizing this process to ensure long-lasting electrodes capable of withstanding multiple cycles of Hg removal and regeneration, while also considering sustainable and cost-effective use of scarce and expensive metals such as Pt. In addition, designing a specific regeneration solution can further improve the regeneration process, while complementary removal methods, such as precipitation, should be explored to effectively recover Hg from the solution for its safe final disposal.

Further investigations into Hg removal in concentrated H_2SO_4 are particularly important, given the urgent need for effective Hg removal methods in concentrated acids. This includes identifying stable electrode materials for such highly corrosive environments, either by continuing research on carbon foams or exploring alternative options. In addition, scaling up the Hg removal process in the concentrated acid, from a medium-scale demonstrator to on-site pilot studies at the mining site, can be a next step. At this stage, identifying materials suitable for the entire pilot system is crucial to ensure long-term Hg removal and corrosion resistance in the concentrated acid.

Another key research direction involves expanding the implementation of the flow reactor system in dental clinics, with the goal of widespread use. In addition, the potential of the flow reactor system for treating various types of wastewater, as well as natural water, can be explored. By broadening the practical applications of this flow reactor system, this technology could become a versatile solution for addressing water pollution in a wide range of industrial and environmental settings.

Electrochemical alloy formation has proven to be a promising method for Hg removal. With further research, optimization, and technological advancements, it holds the potential to become an effective solution for Hg decontamination in various aqueous solutions. Its real-world applications can extend to environmental remediation, industrial wastewater treatment, large-scale decontamination of concentrated acid, and beyond, ultimately contributing to global Hg mitigation efforts.

Acknowledgment

This project was financially supported by the Swedish Research Council for Sustainable Development (Formas). Additional funding was provided by the Strategic Innovation Program Swedish Mining Innovation, supported by the Swedish Agency for Innovation Systems (Vinnova) and the Swedish Energy Agency (Energimyndigheten).

First and foremost, I would like to thank my supervisor, Björn Wickman, for his support, patience, and insightful feedback, which guided me throughout this project. I am also grateful to my co-supervisor, Teodora Retegan Vollmer, for her support and expertise. My sincere thanks go to my examiner, Henrik Grönbeck, for his constructive feedback and valuable insights.

To all the members of the electrochemistry group and the team at Atium, thank you for all the engaging discussions, continuous encouragements, collaborations, and friendship. Finally, I would like to express my heartfelt gratitude to my family and friends, both in Sweden and back home in Iceland.

Bibliography

[1] B. Ericson, J. Caravanos, K. Chatham-Stephens, P. Landrigan and R. Fuller, "Approaches to systematic assessment of environmental exposures posed at hazardous waste sites in the developing world: The toxic sites identification program," *Environmental Monitoring and Assessment*, vol. 185, pp. 1755–1766, 2 2012. DOI: 10.1007/s10661-012-2665-2.

[2] "World's worst pollution problems - the toxics beneath our feet," Pure Earth and Green Cross Switzerland, 2016.

[3] G. Filippelli, S. Anenberg, M. Taylor, A. Geen and H. Khreis, "New approaches to identifying and reducing the global burden of disease from pollution," *GeoHealth*, vol. 4, 4 Apr. 2020. DOI: 10.1029/2018GH000167.

[4] "World's worst pollution problems - the new top six toxic threats: A priority list for remediation," Pure Earth and Green Cross Switzerland, 2015.

[5] *10 chemicals of public health concern*, Jun. 2020. [Online]. Available: https://www.who.int/news-room/photo-story/photo-story-detail/10-chemicals-of-public-health-concern.

[6] "Minamata convention on mercury: Annotated bibliography of who information," World Health Organization, Publications, 2021, iv, 39 p.

[7] N. Pirrone *et al.*, "Global mercury emissions to the atmosphere from natural and anthropogenic sources," in Springer US, 2009, pp. 1–47. DOI: 10.1007/978-0-387-93958-2_1.

[8] "Global mercury assessment," UN Environment Programme, 2018.

[9] D. G. Streets *et al.*, "Total mercury released to the environment by human activities," *Environmental Science Technology*, vol. 51, pp. 5969–5977, 11 2017. DOI: 10.1021/acs.est.7b00451.

[10] L. J. Esdaile and J. M. Chalker, "The mercury problem in artisanal and small-scale gold mining," *Chemistry – A European Journal*, vol. 24, pp. 6905–6916, 27 May 2018. DOI: 10.1002/chem.201704840.

[11] A. K. Saim, "Mercury (hg) use and pollution assessment of asgm in ghana: Challenges and strategies towards hg reduction," *Environmental Science and Pollution Research*, vol. 28, pp. 61 919–61 928, 44 Nov. 2021. DOI: 10.1007/s11356-021-16532-4.

[12] D. O'Connor *et al.*, "Mercury speciation, transformation, and transportation in soils, atmospheric flux, and implications for risk management: A critical review," *Environment International*, vol. 126, pp. 747–761, 2019. DOI: 10.1016/j.envint.2019.03.019.

[13] N. E. Selin, "Global biogeochemical cycling of mercury: A review," *Annual Review of Environment and Resources*, vol. 34, pp. 43–63, 1 Nov. 2009, ISSN: 1543-5938. DOI: 10.1146/annurev.environ.051308.084314.

[14] C. T. Driscoll, R. P. Mason, H. M. Chan, D. J. Jacob and N. Pirrone, "Mercury as a global pollutant: Sources, pathways, and effects," *Environmental Science Technology*, vol. 47, pp. 4967–4983, 10 2013. DOI: 10.1021/es305071v.

[15] P. A. Ariya *et al.*, "Mercury physicochemical and biogeochemical transformation in the atmosphere and at atmospheric interfaces: A review and future directions," *Chemical Reviews*, vol. 115, pp. 3760–3802, 10 2015. DOI: 10.1021/cr500667e.

[16] K. Hua, X. Xu, Z. Luo, D. Fang, R. Bao and J. Yi, "Effective removal of mercury ions in aqueous solutions: A review," *Current Nanoscience*, vol. 16, pp. 363–375, 3 2020. DOI: 10.2174/1573413715666190112110659.

[17] A Sharma and R. K. Arya, "Removal of mercury(ii) from aqueous solution: A review of recent work," *Separation Science and Technology*, vol. 50, pp. 1310–1320, 9 2015. DOI: 10.1080/01496395.2014.968261.

[18] G. Crini and E. Lichtfouse, "Advantages and disadvantages of techniques used for wastewater treatment," *Environmental Chemistry Letters*, vol. 17, pp. 145–155, 1 Mar. 2019. DOI: 10.1007/s10311-018-0785-9.

[19] C. Tunsu and B. Wickman, "Effective removal of mercury from aqueous streams via electrochemical alloy formation on platinum," *Nature Communications*, vol. 9, p. 4876, 1 Nov. 2018. DOI: 10.1038/s41467-018-07300-z.

[20] M. K. O. Bengtsson, C. Tunsu and B. Wickman, "Decontamination of mercury-containing aqueous streams by electrochemical alloy formation on copper," *Industrial Engineering Chemistry Research*, vol. 58, pp. 9166–9172, 21 2019. DOI: 10.1021/acs.iecr.9b01513.

[21] V. Roth *et al.*, "Mercury removal from concentrated sulfuric acid by electrochemical alloy formation on platinum," *ACS EST Engineering*, vol. 3, pp. 823–830, 6 Jun. 2023. DOI: 10.1021/acsestengg.2c00417.

[22] E. Feldt *et al.*, "Temperature and concentration dependence of the electrochemical pthg4 alloy formation for mercury decontamination," *Separation and Purification Technology*, vol. 319, p. 124 033, Aug. 2023. DOI: 10.1016/j.seppur.2023.124033.

[23] W. Fitzgerald and C. Lamborg, "Geochemistry of mercury in the environment," in *Treatise on Geochemistry*, H. D. Holland and K. K. Turekian, Eds., Oxford: Pergamon, 2007, pp. 1–47. DOI: 10.1016/B0-08-043751-6/09048-4.

[24] A. B. Mukherjee, R Zevenhoven, J Brodersen, L. D. Hylander and P Bhattacharya, "Mercury in waste in the european union: Sources, disposal methods and risks," *Resources Conservation and Recycling*, vol. 42, pp. 155–182, 2 2004. DOI: DOI10.1016/j.resconrec.2004.02.009.

[25] L. D. Hylander and R. B. Herbert, "Global emission and production of mercury during the pyrometallurgical extraction of nonferrous sulfide ores," *Environmental Science Technology*, vol. 42, pp. 5971–5977, 16 Aug. 2008. DOI: 10.1021/es800495g.

[26] "Mercury in the artic," Arctic Monitoring and Assessment Programme, 2021.

[27] W. Shotyk, "Arctic plants take up mercury vapour," *Nature*, vol. 547, pp. 167–168, 7662 Jul. 2017. DOI: 10.1038/547167a.

[28] N. Selin, D. Jacob, R. Yantosca, S. Strode, L. Jaeglé and E. Sunderland, "Global 3-d land-ocean-atmosphere model for mercury: Present-day versus preindustrial cycles and anthropogenic enrichment factors for deposition," *Global Biogeochemical Cycles*, vol. 22, Sep. 2008. DOI: 10.1029/2007GB003040.

[29] H. Gonzalez-Raymat *et al.*, "Elemental mercury: Its unique properties affect its behavior and fate in the environment," *Environmental Pollution*, vol. 229, pp. 69–86, Oct. 2017. DOI: 10.1016/j.envpol.2017.04.101.

[30] N. E. Selin, "Mercury rising: Is global action needed to protect human health and the environment?" *Environment: Science and Policy for Sustainable Development*, vol. 47, pp. 22–35, 1 Jan. 2005. DOI: 10.3200/ENVT.47.1.22-37.

[31] M. F. Wolfe, S. Schwarzbach and R. A. Sulaiman, "Effects of mercury on wildlife: A comprehensive review," *Environmental Toxicology and Chemistry*, vol. 17, pp. 146–160, 2 Feb. 1998. DOI: 10.1002/etc.5620170203.

[32] A. Scheuhammer, "The chronic toxicity of aluminium, cadmium, mercury, and lead in birds: A review," *Environmental Pollution*, vol. 46, pp. 263–295, 4 1987. DOI: 10.1016/0269-7491(87)90173-4.

[33] D. Muir, R. Wagemann, B. Hargrave, D. Thomas, D. Peakall and R. Norstrom, "Arctic marine ecosystem contamination," *Science of The Total Environment*, vol. 122, pp. 75–134, 1-2 Jul. 1992. DOI: 10.1016/0048-9697(92)90246-O.

[34] S. M. Ullrich, T. W. Tanton and S. A. Abdrashitova, "Mercury in the aquatic environment: A review of factors affecting methylation," *Critical Reviews in Environmental Science and Technology*, vol. 31, pp. 241–293, 3 2001. DOI: 10.1080/20016491089226.

[35] J.-D. Park and W. Zheng, "Human exposure and health effects of inorganic and elemental mercury," *Journal of Preventive Medicine Public Health*, vol. 45, pp. 344–352, 6 Nov. 2012. DOI: 10.3961/jpmph.2012.45.6.344.

[36] M. Zhao, Y. Li and Z. Wang, "Mercury and mercury-containing preparations: History of use, clinical applications, pharmacology, toxicology, and pharmacokinetics in traditional chinese medicine.," *Frontiers in pharmacology*, vol. 13, p. 807 807, 2022. DOI: 10.3389/fphar.2022.807807.

[37] A. V. Tibau and B. D. Grube, "Mercury contamination from dental amalgam," *Journal of Health and Pollution*, vol. 9, 22 Jun. 2019. DOI: 10.5696/2156-9614-9.22.190612.

[38] T. Y. K. Chan, "Inorganic mercury poisoning associated with skin-lightening cosmetic products," *Clinical Toxicology*, vol. 49, pp. 886–891, 10 Dec. 2011. DOI: 10.3109/15563650.2011.626425.

[39] B. F. Azevedo *et al.*, "Toxic effects of mercury on the cardiovascular and central nervous systems," *Journal of Biomedicine and Biotechnology*, vol. 2012, pp. 1–11, 2012. DOI: 10.1155/2012/949048.

[40] G. Genchi, M. Sinicropi, A. Carocci, G. Lauria and A. Catalano, "Mercury exposure and heart diseases," *International Journal of Environmental Research and Public Health*, vol. 14, p. 74, 1 Jan. 2017. DOI: 10.3390/ijerph14010074.

[41] J. C. Clifton, "Mercury exposure and public health," *Pediatric Clinics of North America*, vol. 54, pp. 237–+, 2 2007, Clifton, Jack C., II 1557-8240. DOI: 10.1016/j.pcl.2007.02.005.

[42] M. Harada, "Minamata disease: Methylmercury poisoning in japan caused by environmental pollution," *Critical Reviews in Toxicology*, vol. 25, pp. 1–24, 1 Jan. 1995. DOI: 10.3109/10408449509089885.

[43] "Guidelines for drinking-water quality, 4th edition, incorporating the 1st addendum," World Health Organization, 2017.

[44] "Council directive 98/83/ec of 3 november 1998 on the quality of water intended for human consumption," European Union, 1998.

[45] T. S. George, "Discovering the disease and its cause," in Harvard University Asia Center, Oct. 2001, pp. 43–70. DOI: 10.1163/9781684173471_005.

[46] K. Eto, "Minamata disease," *Neuropathology*, vol. 20, pp. 14–19, s1 Sep. 2000, ISSN: 0919-6544. DOI: 10.1046/j.1440-1789.2000.00295.x.

[47] H. Kobayashi, "Minamata: How a policy maker addressed a very wicked water quality policy problem," *Water International*, vol. 43, pp. 404–423, 3 Apr. 2018, ISSN: 0250-8060. DOI: 10.1080/02508060.2018.1456192.

[48] O. Rodríguez, I. Padilla, H. Tayibi and A. López-Delgado, "Concerns on liquid mercury and mercury-containing wastes: A review of the treatment technologies for the safe storage," *Journal of Environmental Management*, vol. 101, pp. 197–205, Jun. 2012. DOI: 10.1016/j.jenvman.2012.02.013.

[49] J. Georgin, D. S. P. Franco, Y. Dehmani, P. Nguyen-Tri and N. E. Messaoudi, "Current status of advancement in remediation technologies for the toxic metal mercury in the environment: A critical review," *Science of The Total Environment*, vol. 947, p. 174 501, Oct. 2024. DOI: 10.1016/j.scitotenv.2024.174501.

[50] J. Patterson, E. Barth and L. Stein, "Aqueous mercury treatment," U.S. Environmental Protection Agency, Jul. 1997.

[51] J. G. Yu *et al.*, "Removal of mercury by adsorption: A review," *Environmental Science and Pollution Research*, vol. 23, pp. 5056–5076, 6 2016. DOI: 10.1007/s11356-015-5880-x.

[52] F. L. Fu and Q Wang, "Removal of heavy metal ions from wastewaters: A review," *Journal of Environmental Management*, vol. 92, pp. 407–418, 3 2011. DOI: 10.1016/j.jenvman.2010.11.011.

[53] M. Taseidifar, F. Makavipour, R. M. Pashley and A. M. Rahman, "Removal of heavy metal ions from water using ion flotation," *Environmental Technology Innovation*, vol. 8, pp. 182–190, 2017. DOI: https://doi.org/10.1016/j.eti.2017.07.002.

[54] J. A. Ritter and J. P. Bibler, "Removal of mercury from waste-water - large-scale performance of an ion exchange process," *Water Science and Technology*, vol. 25, pp. 165–172, 3 1992.

[55] V. Roth *et al.*, "On the mechanism and energetics of electrochemical alloy formation between mercury and platinum for mercury removal from aqueous solutions," *Electrochimica Acta*, vol. 507, p. 145 137, Dec. 2024, ISSN: 00134686. DOI: 10.1016/j.electacta.2024.145137.

[56] C. H. Hamann, A. Hamnett and W. Vielstich, *Electrochemistry*, 2nd. WILEY-VCH, 2007, p. 550.

[57] G. Jerkiewicz, "Standard and reversible hydrogen electrodes: Theory, design, operation, and applications," *ACS Catalysis*, vol. 10, pp. 8409–8417, 15 Aug. 2020. DOI: 10.1021/acscatal.0c02046.

[58] A. Gross, "Reversible vs standard hydrogen electrode scale in interfacial electrochemistry from a theoretician's atomistic point of view," *The Journal of Physical Chemistry C*, vol. 126, pp. 11 439–11 446, 28 Jul. 2022. DOI: 10.1021/acs.jpcc.2c02734.

[59] R. G. Compton and C. E. Banks, *Understanding Voltammetry*, 3rd ed., H. Moses, J. Brough and K. S. Ying, Eds. Word Scientific Publishing Europe Ltd., 2018.

[60] C. Gumiński, "Review selected properties of simple amalgams," *Journal of Materials Science*, vol. 24, pp. 2661–2676, 8 Aug. 1989. DOI: 10.1007/BF02385609.

[61] C Guminski, "The hg-pt (mercury-platinum) system," *Bulletin of Alloy Phase Diagrams*, vol. 11, pp. 26–32, 1 1990. DOI: 10.1007/bf02841581.

[62] S. K. Lahiri and D. Gupta, "A kinetic study of platinum-mercury contact reaction," *Journal of Applied Physics*, vol. 51, pp. 5555–5560, 10 1980. DOI: 10.1063/1.327440.

[63] F. L. Fertonani, A. V. Benedetti and M Ionashiro, "Contribution to the study of the reaction of mercury with platinum and a platinum-iridium alloy," *Thermochimica Acta*, vol. 265, pp. 151–161, 1995. DOI: http://dx.doi.org/10.1016/0040-6031(95)02417-Z.

[64] G. R. Souza, I. A. Pastre, A. V. Benedetti, C. A. Ribeiro and F. L. Fertonani, "Solid state reactions in the platinum–mercury system thermogravimetry and differential scanning calorimetry," *Journal of Thermal Analysis and Calorimetry*, vol. 88, pp. 127–132, 2007. DOI: 10.1007/s10973-006-8037-9.

[65] H. Okamoto and T. B. Massalski, "The au-hg (gold-mercury) system," *Bulletin of Alloy Phase Diagrams*, vol. 10, pp. 50–58, 1 Feb. 1989, ISSN: 0197-0216. DOI: 10.1007/BF02882176.

[66] Q. ul-ain khan *et al.*, "Synthesis and mechanical properties of dental amalgam," *Materials Today: Proceedings*, vol. 47, S33–S37, 2021. DOI: 10.1016/j.matpr.2020.04.672.

[67] U. G. Bengtsson and L. D. Hylander, "Increased mercury emissions from modern dental amalgams," *BioMetals*, vol. 30, pp. 277–283, 2 Apr. 2017. DOI: 10.1007/s10534-017-0004-3.

[68] W. Gunnar, "Metal foams for electrodes," Fraunhofer IFAM, 2022.

[69] E. Aerospace, *Carbon (rvc) foam.* [Online]. Available: https://ergaerospace.com/carbon-rvc-foam-open-cell-material/.

[70] P. Westbroek, "Fundamentals of electrochemistry," in Elsevier, 2005, pp. 3–36. DOI: 10.1533/9781845690878.1.1.

[71] T. Biegler, D. Rand and R. Woods, "Limiting oxygen coverage on platinized platinum; relevance to determination of real platinum area by hydrogen adsorption," *Journal of Electroanalytical Chemistry and Interfacial Electrochemistry*, vol. 29, no. 2, pp. 269–277, 1971.

[72] D. A. Buttry and M. D. Ward, "Measurement of interfacial processes at electrode surfaces with the electrochemical quartz crystal microbalance," *Chemical Reviews*, vol. 92, pp. 1355–1379, 6 1992. DOI: 10.1021/cr00014a006.

[73] S. Nilsson, F. Björefors and N. D. Robinson, "Electrochemical quartz crystal microbalance study of polyelectrolyte film growth under anodic conditions," *Applied Surface Science*, vol. 280, pp. 783–790, Sep. 2013. DOI: 10.1016/j.apsusc.2013.05.062.

[74] E. J. Calvo and R. Etchenique, "Kinetic applications of the electrochemical quartz crystal microbalance (eqcm)," in 1999, pp. 461–487. DOI: 10.1016/S0069-8040(99)80017-X.

[75] M. Edvardsson, "Dissipation, what it is, why it is important, and how to measure it," Biolin Scientific.

[76] G. Sauerbrey, "Verwendung von schwingquarzen zur wägung dünner schichten und zur mikrowägung," *Zeitschrift für Physik*, vol. 155, pp. 206–222, 2 Apr. 1959. DOI: 10.1007/BF01337937.

[77] "Qcm-d data analysis," Biolin Scientific.

[78] S. Wilschefski and M. Baxter, "Inductively coupled plasma mass spectrometry: Introduction to analytical aspects," *Clinical Biochemist Reviews*, vol. 40, pp. 115–133, 3 Aug. 2019. DOI: 10.33176/AACB-19-00024.

[79] R. Thomas, *Practical Guide to ICP-MS and Other Atomic Spectroscopy Techniques*, 4th. CRC Press, 2023.

[80] C. F. Harrington, S. A. Merson and T. M. D. Silva, "Method to reduce the memory effect of mercury in the analysis of fish tissue using inductively coupled plasma mass spectrometry," *Analytica Chimica Acta*, vol. 505, pp. 247–254, 2 Mar. 2004. DOI: 10.1016/j.aca.2003.10.046.

[81] B. M. W. Fong, T. S. Siu, J. S. K. Lee and S. Tam, "Determination of mercury in whole blood and urine by inductively coupled plasma mass spectrometry," *Journal of Analytical Toxicology*, vol. 31, pp. 281–287, 5 Jun. 2007. DOI: 10.1093/jat/31.5.281.

[82] J. L. Rodrigues *et al.*, "Determination of total and inorganic mercury in whole blood by cold vapor inductively coupled plasma mass spectrometry (cv icp-ms) with alkaline sample preparation," *Journal of Analytical Atomic Spectrometry*, vol. 24, pp. 1414–1420, 10 2009. DOI: 10.1039/b910144f.

[83] Y. Li *et al.*, "Elimination efficiency of different reagents for the memory effect of mercury using icp-ms," *Journal of Analytical Atomic Spectrometry*, vol. 21, pp. 94–96, 1 2006. DOI: 10.1039/b511367a.

[84] R. S. Pappas, "Sample preparation problem solving for inductively coupled plasma-mass spectrometry with liquid introduction systems i. solubility, chelation, and memory effects.," *Spectroscopy (Springfield, Or.)*, vol. 27, pp. 20–31, 5 May 2012.

[85] M. Korvela, M. Andersson and J. Pettersson, "Internal standards in inductively coupled plasma mass spectrometry using kinetic energy discrimination and dynamic reaction cells," *Journal of Analytical Atomic Spectrometry*, vol. 33, pp. 1770–1776, 10 2018. DOI: 10.1039/C8JA00171E.

[86] "Dma-80 direct mercury analyzer," Milestone.

[87] B. Inkson, "Scanning electron microscopy (sem) and transmission electron microscopy (tem) for materials characterization," in Elsevier, 2016, pp. 17–43. DOI: 10.1016/B978-0-08-100040-3.00002-X.

[88] A. A. Bunaciu, E. gabriela Udriştioiu and H. Y. Aboul-Enein, "X-ray diffraction: Instrumentation and applications," *Critical Reviews in Analytical Chemistry*, vol. 45, pp. 289–299, 4 Oct. 2015. DOI: 10.1080/10408347.2014.949616.

[89] R. Bharti, K. Wadhwani, A. Tikku and A. Chandra, "Dental amalgam: An update," *Journal of Conservative Dentistry*, vol. 13, p. 204, 4 2010. DOI: 10.4103/0972-0707.73380.

[90] H. Stripple, M. Nerentorp and I. Wängberg, "Environmental and technical evaluation with life cycle assessment hg-rid-life mercury decontamination of dental care facilities," Tech. Rep., Aug. 2019.

[91] C. D. Lynch, D. J. J. Farnell, H. Stanton, I. G. Chestnutt, P. A. Brunton and N. H. F. Wilson, "No more amalgams: Use of amalgam and amalgam alternative materials in primary dental care," *British Dental Journal*, vol. 225, pp. 171–176, 2 Jul. 2018. DOI: 10.1038/sj.bdj.2018.538.

[92] *Global overview of countries phasing out dental amalgam*, EnvMed Network, 2024. [Online]. Available: https://environmentalmedicine.eu/mercury-free-dentistry-for-planet-earth/.

[93] M. Cataldi, "Dental unit wastewater, a current environmental problem: A sistematic review," *Oral Implantology*, vol. 10, p. 354, 4 2017. DOI: 10.11138/orl/2017.10.4.354.

[94] J. L. Drummond, M. D. Cailas and K. Croke, "Mercury generation potential from dental waste amalgam," *Journal of Dentistry*, vol. 31, pp. 493–501, 7 Sep. 2003, ISSN: 03005712. DOI: 10.1016/S0300-5712(03)00083-6.

[95] L. D. Hylander, A. Lindvall and L. Gahnberg, "High mercury emissions from dental clinics despite amalgam separators," *Science of The Total Environment*, vol. 362, pp. 74–84, 1-3 Jun. 2006, ISSN: 00489697. DOI: 10.1016/j.scitotenv.2005.06.008.

[96] M. E. Stone, M. E. Cohen, D. L. Berry and J. C. Ragain, "Design and evaluation of a filter-based chairside amalgam separation system," *Science of The Total Environment*, vol. 396, pp. 28–33, 1 Jun. 2008. DOI: 10.1016/j.scitotenv.2008.02.037.

[97] M. E. Stone, "The effect of amalgam separators on mercury loading to wastewater treatment plants.," *Journal of the California Dental Association*, vol. 32, pp. 593–600, 7 Jul. 2004, ISSN: 1043-2256.

[98] H. Binner, N. Kamali, M. Harding and T. Sullivan, "Characteristics of wastewater originating from dental practices using predominantly mercury-free dental materials," *Science of The Total Environment*, vol. 814, p. 152 632, Mar. 2022. DOI: 10.1016/j.scitotenv.2021.152632.

[99] M. J. King, W. G. Davenport and M. S. Moats, *Metallurgical offgas cooling and cleaning*, 2013. DOI: 10.1016/B978-0-08-098220-5.00004-6.

[100] "Mineral commodity summaries," US Geological Survey, 2022. DOI: 10.3133/mcs2022.

[101] "Sulphur products," Boliden, 2018.

[102] Q. Wu *et al.*, "New insight into atmospheric mercury emissions from zinc smelters using mass flow analysis," *Environmental Science Technology*, vol. 49, pp. 3532–3539, 6 Mar. 2015. DOI: 10.1021/es505723a.

[103] Z. Liu *et al.*, "Transport and transformation of mercury during wet flue gas cleaning process of nonferrous metal smelting," *Environmental Science and Pollution Research*, vol. 24, pp. 22 494–22 502, 28 Oct. 2017. DOI: 10.1007/s11356-017-9852-1.

[104] F. Roger, "The performance of stainless steels in concentrated sulphuric acid," Stainless Steel World, 2009.